C.P. No. 449
(19,900)
A.R.C. Technical Report

C.P. No. 449
(19,900)
A.R.C. Technical Report

MINISTRY OF SUPPLY

AERONAUTICAL RESEARCH COUNCIL

CURRENT PAPERS

Stall Cell Propagation in Two Mismatched Compressor Stages

by

R. C. Turner, T. J. Hargest and R. A. Burrows

LONDON: HER MAJESTY'S STATIONERY OFFICE

1959

Price 5s. 6d. net

C.P.No.449

U.D.C. No. 621.438.031.3:621.004.63

Memorandum No. M.313

NATIONAL GAS TURBINE ESTABLISHMENT

January, 1958

Stall cell propagation in two mismatched compressor stages

- by -

R. C. Turner, T. J. Hargest and R. A. Durrows

SUMMARY

This Memorandum describes an investigation into the flow fluctuations occurring in two mismatched stages in the N.G.T.E. 106 low speed compressor. Its purpose is to contribute to a general understanding of surging and unsteady flow phenomena in full scale compressors when operating in a mismatched condition.

Hot wire anemometers were used to examine the fluctuations, measurements being made before and after each blade row at seven flow coefficients.

It was found that before surge was reached, random fluctuations of amplitude up to nearly 30 per cent of the mean velocity occurred, the amplitude tending to increase as surge was approached. The major surge consisted of a single stall cell rotating at 35 per cent of the compressor speed but this was preceded by a less noticeable surge which consisted of three cells rotating at the same speed. The flow in the annulus outside the stall cells was found to have a cyclic distribution, with an amplitude of the order of 50 per cent of the mean velocity, the cells occurring in the regions of lowest velocity.

The results generally emphasise the complex nature of the flows occurring in the surge and near surge conditions, and the dependence of stall cell propagation in one stage on interference from neighbouring stages.

CONTENTS

APPENDICES

ILLUSTRATIONS

Fig. No.	Title
1	Assembly of compressor
2	Blade spacing and anemometer positions
3	Circuit and anemometer details
4	Characteristics - stages tested in series
5	Characteristics - stages tested separately
6	Effect of amplifier distortion on typical stall cell record
7	Anemometer records - two-stage build; $Va/U = 0.55$
8	Anemometer records - two-stage build; $Va/U = 0.51$
9	Anemometer records - two-stage build; $Va/U = 0.46$
10	Anemometer records - two-stage build; $Va/U = 0.35$
11	Anemometer records - two-stage build; $Va/U = 0.285$
12	Anemometer records - two-stage build; $Va/U = 0.25$
13	Anemometer records - two-stage build; $Va/U = 0$
14	Anemometer records - single-stage build; $Va/U = 0.55$ and 0.51
15	Anemometer records - single-stage build; $Va/U = 0.46$ and 0.35
16	Anemometer records - single-stage build; $Va/U = 0.285$ and 0.25
17	Anemometer records - single-stage build; $Va/U = 0$
18	Stall cell characteristics of slow pulse surge
19	Two-stage tests effect of inter-stage spacing on surge flow coefficient

1.0 Introduction

The work described in this Memorandum is part of a general examination of compressor surge, and is a continuation of the investigation reported in Reference 1. This reference reports tests on the effect of inter-stage spacing on the surge behaviour of two mismatched compressor stages, of which the second had the lower surge flow coefficient when tested separately. At the smallest spacing of the tests, the stages surged at the separate surge flow of the second stage, the surges of the separate and of the combined stages all producing a similar sound, a steady pulsation of approximately 10 c/sec.

At a somewhat higher inter-stage spacing a secondary surge was observed to precede the main surge; it was characterised by a more rapid pulsation and resulted in a smaller discontinuity in the pressure rise characteristics. For convenience this secondary surge is referred to as the "rapid pulse" surge as distinct from the primary or "slow pulse" surge.

The object of the present investigation was to make a detailed examination of the flow fluctuations associated with the various surge conditions in the two-stage tests at the higher spacing, a similar examination being carried out on the first stage when tested alone, for purposes of comparison.

2.0 Apparatus

2.1 The compressor

The 106 compressor is described in Reference 2. It is a low speed multi-stage machine of constant annulus dimensions and a diameter ratio of 0.75. The blade height is 2.5 in. and the mean diameter 17.5 in. At the normal running speed of 1500 rev/min, the mean diameter blade speed is 114.5 ft/sec, and the blade Reynolds number based on this speed and the blade chord is 0.65×10^5. The blade chord is approximately 1.1 in. and the mean diameter pitch/chord ratio is 0.85. Any number of stages up to eight can be employed and the inter-stage spacing can be varied within limits.

In the present tests, the blades were of medium stagger free vortex design with 50 per cent reaction at mean diameter. Design details of Stage 1 are given in Appendix I. For Stage 2, the stagger of both rotor and stator blades was numerically increased by 15°; the axial spacing between Stage 1 stator blades and Stage 2 rotor blades was approximately five blade chords.

Figure 1 shows the general arrangement of the compressor assembled with two stages and Figure 2 the leading dimensions of the blading.

2.2 Hot wire anemometers

Two hot wire anemometers, 132° apart, were placed before and after each stator blade row as shown in Figure 2. An additional anemometer was placed after the first-stage rotor blade row. Figure 2 also gives the identification code for the anemometer positions. Each anemometer could be traversed across the blade passage; for these tests, three radial positions were selected, 0.5 in. from the outside diameter, 0.5 in. from the inside diameter, and mean diameter.

The active element of the anemometer consisted of a tungsten wire 0.0004 in. in diameter, and 0.08 in. long, of approximately 2 ohms resistance at room temperature, soldered across pin supports, as shown in Figure 3. The supply and measuring circuit is also shown in Figure 3. The wire heating current, drawn from lead acid accumulators of large capacity, was effectively constant and was adjusted so that a fixed ratio was maintained between the mean resistance of the element when it was hot and when it was at the temperature of the air flow. Under these conditions the output from the hot wire could be interpreted. The outputs were recorded by means of a six-channel cathode ray recording unit.

The simplified theory of the hot wire anemometer is dealt with in Appendix II.

2.3 Other measurements

Mass flow was calculated from the velocity head in the outlet ducting, measured sufficiently far downstream to be unaffected by the surge flow fluctuations. A calibration was derived in the unsurged condition from the inlet static depression, which possessed a known relationship to the mass flow. This relationship had been found not to apply during surge, and thus could not be used directly in the present tests.

Temperature was measured at inlet by means of a mercury-in-glass thermometer, and speed with a Hasler hand tachometer.

The aerodynamic characteristics of the blading had already been determined and reported in Reference 1, but check pressure measurements were taken during the present tests by means of pitot combs placed after each stage

3.0 Test technique

The two-stage build was tested first, the flow fluctuations being recorded at all positions, at each of seven flow coefficients. The compressor was then rebuilt with the first stage only, and the tests were repeated at the same flow coefficients, the anemometers at position 'B' in Figure 2 being omitted.

The flow coefficients of the tests were selected with reference to the aerodynamic characteristics of the stages as reported in Reference 1. Figure 4 shows the characteristics as obtained in the two stages when tested together and Figure 5 those for the stages tested individually the flow coefficients of the present tests also being indicated. A description of the noise emitted is given at the top of the figures, the hatched areas representing the surge discontinuities.

The anemometers were yawed so that the tungsten wire was at right angles to the axial direction. Thus the fluctuations measured were substantially those of the axial component of the velocity.

The following table relates the positions of the test flow coefficients to the flow conditions of the compressor.

Va/U	Remarks	
	Stages 1 and 2 in series	Stage 1 only
0.55	Unsurged	Unsurged
0.51	Unsurged	Unsurged; near start of slow pulse surge
0.46	Unsurged; near start of rapid pulse surge	Slow pulse surge starts
0.35	Rapid pulse surge	Slow pulse surge
0.285	Slow pulse surge starts	Slow pulse surge
0.25	Slow pulse surge	Slow pulse surge
0.0	Slow pulse surge	Slow pulse surge

4.0 Test results

4.1 General

As described in Section 2.2, records were taken at three radial positions. Within the general limits of accuracy of the tests it was found that the mean diameter conditions were sufficiently representative of those over the whole blade height. The comments in this section and the records reproduced in Figures 7 to 17 are therefore confined to the mean diameter conditions.

In all the records, the lower trace was provided by a tachometer generator, one cycle representing one revolution of the compressor rotor, i.e. 0.04 seconds in these tests. On the remaining traces, positive velocity increments are measured downwards.

The anemometer positions for each trace are indicated in the Figures, the numbering system being shown in Figure 2.

4.2 Accuracy of records

There are several factors which prevent the records from being exact (i.e. linear) representations of the time variation of the air velocity at the hot wire. The first of these is that the relationship between change of velocity and change of wire resistance is linear for small changes only (see Appendix II); those experienced in these tests were comparatively large. Also, if the fluctuations are so large as to reverse the direction of flow, the reverse velocity is shown on the records as being of positive sign, the hot wire responding to magnitudes only.

Another factor is that the response of a hot wire diminishes with increase of frequency of the imposed velocity fluctuations. This is because of the lag caused by heat storage in the wire. It is discussed briefly in Appendix II. There is also an accompanying phase change.

Finally, the frequency response of the amplifiers may distort the records. This was the major cause of distortion in the present tests. Ideally, the amplifiers should be such as to just compensate for frequency response of the hot wire. With the amplifiers available for the present tests, however, the lowest frequency components of the velocity fluctuations were recorded on a scale of the order of one tenth of that of the highest frequencies. Figure 6 has been prepared to illustrate this distortion. In the upper diagram a typical record of a stall cell is shown while the lower diagram shows the same record with an approximate correction made for the amplitude distortion. Another kind of distortion which may be present is a phase shift between the high and low frequency components, this resulting in an incorrect positioning of the high frequency region in Figure 6 in relation to the low frequency component. The high frequency region, which is the actual stall cell, should be shifted towards the trough of the low frequency component.

4.3 Types of record obtained

The records are described in detail in the succeeding sections; they can be divided into two main categories - random perturbations and rotating stall cells. Perturbations in the velocity occur at flows considerably larger than the surge flow; they appear to be completely irregular, as regards timing, amplitude, and distribution in the annulus. Blade wakes can be detected on the records as a high frequency fluctuation. It is shown in succeeding sections that rotating stall cells occurred whenever the compressor was surged; they were detected by comparing the records of two or more anemometers spaced round the annulus.

The lower diagram of Figure 6 shows a typical stall cell record corrected for amplifier distortion. It consists essentially of two parts - the actual stall cell indicated by the complex region of high frequency fluctuations, and the low frequency swing on which the cell is superimposed. This low frequency swing indicates that even where the blades are unstalled, there is a considerable variation of velocity with circumferential position at any instant, or with time at any position. The internal structure of the stall cell is seen to be complex. The variations of axial velocity are probably due to interaction of stalled blade wakes, and represent changes in both magnitude and direction of velocity, modified by turbulence effects.

Examination of the records shows that in most cases, there is a variation of characteristics (width, amplitude, shape etc.) from stall cell to stall cell, and in the same stall cell as it travels round the annulus. A theoretical concept of a stall cell as an invariable region of reduced velocity and simple shape travelling uniformly round an annulus containing otherwise undisturbed flow would thus be highly simplified.

4.4 Two-stage tests - details of records

In the following sections the amplitudes quoted are measured from the negative peaks to the positive peaks, and are expressed in terms of the mean axial velocity. Because of the general irregularity of the traces, the values quoted are necessarily approximate and represent orders of

magnitude; in the case of stall cells they refer to the low frequency swing only.

$Va/_U$ = 0.55 (Figures 4 and 7)

This is a point well out of surge. Both blade wakes and larger perturbations at irregular intervals can be detected. The wakes are represented by variations of about 1 per cent of the mean axial velocity, while the perturbations are of 3 to 4 per cent magnitude, at all anemometer positions.

$Va/_U$ = 0.51 (Figures 4 and 8)

At this flow, the compressor is still well out of surge. Here again the blade wakes are of about 1 per cent magnitude, with random perturbations of 3 to 5 per cent.

$Va/_U$ = 0.46 (Figures 4 and 9)

This point is near the onset of the rapid pulse surge. The blade wakes are of about 2 per cent magnitude; the perturbations still appear to be random, and have increased in amplitude to 10 per cent after the first-stage rotor, 20 per cent after the first-stage stator, and 4 per cent after the second-stage rotor and stator. The perturbations are thus greatest in the first stage which is operating at a flow lower than its single-stage surge value (Figure 5).

$Va/_U$ = 0.35 (Figures 4 and 10)

At this flow, the rapid pulse surge is occurring. The records show this to consist of three stall cells rotating at 35 per cent of the rotor speed, in the same direction as that of the rotor, and of 20 per cent amplitude. They extend through both stages, but vary in shape from point to point in the same stage and from stage to stage. The stall cell width is approximately 90°.

$Va/_U$ = 0.285 (Figures 4 and 11)

At this flow, the slow pulse surge is fully established. The records show that it consists of one stall cell rotating at 36 per cent of the rotor speed. The amplitude is approximately 50 per cent after the first rotor row, 30 per cent after the first stator, 30 per cent after the second rotor and 50 per cent after the second stator. The stall cell width is rather variable, but after the first-stage stator, a typical value is 185°, and after the second-stage stator, 140°.

$Va/_U$ = 0.25 (Figures 4 and 12)

The single stall cell persists at this flow, the rotational speed being about 34 per cent of the rotor speed. The amplitude is about 50 per cent at all positions; the stall cell width is about 180° after the first stator blade row and 145° after the second stator row. The stall cell shape is still irregular and complex.

$Va/_U$ = 0 (Figures 4 and 13)

This is the closed throttle position and is included for completeness; the conditions in the compressor will obviously be far removed from the

normal condition of predominantly axial flow, and the records given by the hot wire anemometers are of doubtful significance, since no indication of flow direction is given. The records indicate perturbations of 35 to 40 per cent amplitude; there is no definite stall cell pattern. The compressor emitted audible pulsations however, these being probably connected with the increases in amplitude which occur at about every three revolutions (see the lower two traces in Figure 13) and which represent the final state of the stall cells.

4.5 Single-stage tests - details of records

The general remarks at the beginning of the previous section also apply to the single-stage tests.

$Va/U = 0.55$ (Figures 5 and 14)

At this flow the compressor is not surged, but is near the peak of the pressure rise characteristic. The records show random perturbations of about 3 per cent amplitude with blade wakes of 1 to 2 per cent.

$Va/U = 0.51$ (Figures 5 and 14)

This is a point on the low flow side of the peak of the pressure rise characteristic, and is situated just before the onset of surge. The perturbations have increased to 5 to 6 per cent amplitude; the blade wakes are again of 1 to 2 per cent amplitude.

$Va/U = 0.46$ (Figures 5 and 15)

At this flow the surge of the stage has commenced. The records show one stall cell rotating at 35 per cent of the rotor speed, the cell width being approximately 93°; the amplitude of the low frequency swing is 50 per cent. The stall cell structure is again complex.

$Va/U = 0.35$ (Figures 5 and 15)

The single stall cell persists rotating at 36 per cent of the rotor speed. The amplitude is of the same order as before but the width has increased to 142°.

$Va/U = 0.25$ (Figures 5 and 16)

At this flow, the stall cell speed is 35 per cent of the rotor speed; the low frequency swing amplitude varies between 55 per cent and 70 per cent, depending on the anemometer position. The cell width is now about 163°.

$Va/U = 0.25$ (Figures 5 and 16)

There is little change in the low frequency amplitudes but the stall cell width has increased to about 200°. The speed of rotation is 34 per cent of the rotor speed.

$Va/U = 0$ (Figures 5 and 17)

As in the two-stage build at zero flow, the stall cells have disappeared and have been replaced by random perturbations, the magnitude being 20 to 35 per cent. After the stator blades there are indications

of a comparatively regular periodic increase in amplitude, this probably being responsible for the audible pulsations and representing the final state of the stall cells.

5.0 Discussion

Summarising the foregoing, the tests show that at flows prior to surge, the first sign of irregularity in the flow conditions is the occurrence of random perturbations of velocity, these increasing in magnitude as surge is approached. There is no indication of the presence of these perturbations shown in the pressure rise characteristics, at least within the limits of accuracy of the tests on Reference 1; there are for instance no discontinuities to be seen. When surge occurs the rotating stall cells are suddenly established with accompanying discontinuities in the pressure rise characteristics. The stall cells occupy the whole blade height and extend through all blade rows. The "rapid pulse" surge of the two-stage tests consists of three stall cells rotating at 35 per cent of the rotor speed and occurs at flows where the first stage tested alone shows a single stall cell surge, and the second stage tested alone is unsurged. The "slow pulse" surge in both single and two-stage tests consists of one cell rotating at approximately the same speed, which, as in the case of the rapid pulse surge, is substantially constant for all flows.

The records show that the internal structure, i.e. the velocity profile, of a stall cell is complex and varies not only from blade row to blade row but also at different points after the same blade row. Apart from the stall cell itself, the flow in the remainder of the annulus is considerably distorted from the pre-surge uniform distribution; this distortion has been called a "low frequency swing" in this Memorandum, the stall cell occurring in the minimum velocity region.

The effect of reduction of flow coefficient on the low frequency swing amplitude and width of the stall cells in the slow pulse surge condition is illustrated in Figure 18. In the single-stage tests, although the amplitude of the low frequency swing tends to remain constant, the stall cell width increases uniformly; this latter curve has been extrapolated to 360° at zero flow, on the assumption that at zero flow the cell extends over the whole circumference. This assumption is not, however, regarded as possessing universal validity. For the two-stage tests there are insufficient points to justify any general conclusion on changes of the stall cell with changes of flow coefficient; but considering conditions after the first stator blade row, at a flow coefficient of 0.25, the cell width and the amplitude of the low frequency swing are reasonably similar in both the single and two-stage tests. The presence of the second stage operating at a flow coefficient at which it is surged when tested alone, has apparently had little effect on the first-stage conditions.

In none of the tests is there any indication of the attenuation of the stall cells through the second stage; this might for instance have been expected at a flow coefficient of 0.35, where in the single-stage tests the first stage exhibits a single stall cell and the second stage is unsurged. Instead, three stall cells extend through both stages without observable attenuation (Figure 10). Unpublished work at N.G.T.E., however, has shown that in certain cases of mismatching of multi-stage compressors, such attenuation can occur; it is probably a function chiefly of the degree and distribution of mismatching through the stages, the required conditions being unfulfilled in the present tests.

There is at present no generally accepted theory on the factors

governing the number of stall cells in an annulus. Figure 19, which is based on earlier tests reported in Reference 1, shows the effect of variation of inter-stage axial spacing on the rapid pulse and slow pulse surge flow coefficients. It is probable that in all cases the rapid pulse surge was caused by three stall cells, and the slow pulse surge by a single cell. At the lowest and highest spacings the three cell condition did not occur. It is thus apparent that the occurrence of any given stall cell configuration depends partly on the inter-stage spacing, although there are probably several other important factors. It also follows that single-stage tests are probably of little value in the assessment of stall cell propagation in a multi-stage compressor. This has an important bearing on the planning of future research work. It has been observed on this compressor, in tests using up to six stages of conventional blading with normal axial spacings in both matched and moderately mismatched conditions, that at the flow generally recognised as the surge flow, audible pulsations, similar to those of the slow pulse surge, are heard (see for instance Reference 3). The present tests thus suggest that the usual surge on this compressor is associated with a single rotating stall cell.

The present tests do not suggest any criterion for the inception of stall cell regimes. Reference 4 however concludes that stall cells occur when the slope of the overall pressure rise versus flow coefficient curve becomes zero or positive; this is of course a well known criterion for one-dimensional stability in compressors, and is developed for instance in Reference 5. This conclusion is based on single-stage tests. Examination of Figure 5 does not support this theory for the present stages when tested separately; surge is seen to occur for both stages at a lower flow than that corresponding to the peak pressure rise. Figure 4 shows that the rapid pulse surge apparently causes a discontinuity in the overall characteristics of the two stages in series but there is no indication of a significant change of slope prior to this. The inception of the slow pulse surge occurs after the overall characteristic has already exhibited a small positive slope. The results obtained in this region (i.e. when the rapid pulse surge is present) should be treated with reserve however, as the stall cells probably affect the measurements of pressure rise to some extent.

6.0 Conclusions

A stage of free vortex blading has been tested in series with a similar but re-staggered stage, and alone. In the two-stage tests the stagger of the second stage was such as to give a lower surge flow when tested individually, the inter-stage spacing being approximately five blade chords. The flow fluctuations associated with the various surge or near surge conditions were examined by means of hot wire anemometers.

It was found that at flows prior to the first recognisable surge to occur, random perturbations in the flow occurred, increasing in amplitude as the flow coefficient was reduced; the highest amplitude was recorded in the two-stage tests and was about 30 per cent of the mean flow velocity.

In the two-stage tests, the first surge to occur, described in Reference 1 as the "rapid pulse surge", was found to consist of three stall cells rotating at approximately 35 per cent of the compressor rotor speed. At a lower flow, this changed abruptly to the "slow pulse surge", which consisted of a single stall cell rotating at about the same speed; at all conditions the stall cells extended through both stages, and over the whole blade height. The slow pulse surge resulted in a much larger

discontinuity in the pressure rise characteristics than did the rapid pulse surge. In the single-stage tests, the rapid pulse surge did not occur; but the slow pulse surge again consisted of a single cell rotating at about the same speed.

The cells themselves appeared as regions of complex and variable velocity distribution, but externally to them the circumferential distribution of velocity was cyclic, with an amplitude of the order of 50 per cent of the mean velocity, the cells occurring in the regions of lowest velocity. In the single-stage tests, reduction of flow coefficient tended to increase the stall cell width, without much change of the amplitude of the velocity distribution outside the cell.

The investigation generally, taken in conjunction with that of Reference 1, serves to emphasise the importance of inter-stage spacing and stage mismatching as contributory factors deciding the occurrence and type of stall cells and also indicates that single-stage tests would be of little direct assistance in the assessment of stall cell propagation in a multi-stage compressor.

ACKNOWLEDGEMENT

The authors are indebted to Mr. R. Chaplin for assistance in presenting the theory of the hot wire anemometer given in Appendix II, and for general advice during the running of the tests.

NOTATION

U	blade speed
Va	axial velocity
ΔP	total pressure rise
ρ	density

REFERENCES

No.	Author(s)	Title, etc.
1	R. C. Turner	The effect of axial spacing on the surge characteristics of two mismatched axial compressor stages. C.P.431. November, 1956.
2	R. A. Jeffs	Description of the low speed compressor No. 106. A.R.C.6842. April, 1946.
3	A. G. Smith P. J. Fletcher	Observations on the surging of various low speed fans and compressors. A.R.C.17,139. July, 1954.
4	Eleanor L. Costilow Merle C. Huppert	Some effects of guide vane turning and stators on the rotating stall characteristics of a high hub-tip ratio single stage compressor. N.A.C.A. Technical Note 3711, April, 1956.
5	Robert C. Bullock, Ward W. Wilcox Jason J. Moses	Experimental and theoretical studies of surging in continuous flow compressors. N.A.C.A. Report No. 86, 1946.
6	L. V. King	On the convention of heat from small cylinders. Phil. Trans. Royal Society (A), Vol. 214, No. 14, 1914.
7	J. B. Willis	Review of hot wire anemometry. Australian council for Aeronautics. Report ACA-19. October, 1945.
8	Carl E. Pearson	Measurement of instantaneous vector air velocity by hot wire methods. Journal of the Aeronautical Sciences. Volume 19, No. 2, February, 1952.
9	Leslie S. G. Kovasznay	Development of turbulence-measuring equipment. N.A.C.A. Report No. 1209, 1954.

APPENDIX I

Blade design details

The blades were of free vortex design (design flow coefficient = 0.667; 50 per cent reaction at mean diameter), with details as below. The section was C4 on circular arc camber lines; the blade height was 2.5 in. and the mean radius 8.75 in.

The rotor has fifty-eight blades and the stator sixty so that with blade chords of 1.14, 1.10 and 1.06 in. at root, mean and tip respectively, the details are as follows:-

Rotor			
r/rm	0.874	1.0	1.14
β_1	39.2	46.5	50.6
β_2	-3.5	15.6	32.0
θ	42.7	30.9	18.6
s/c	0.726	0.862	1.020
t/c	0.12	0.10	0.08
α_2	5.5	23.4	37.8
Stator			
r/rm	0.860	1.0	1.125
β_3	52.0	46.1	42.2
β_4	18.6	15.9	14.0
θ	33.4	30.2	28.2
s/c	0.744	0.833	0.905
t/c	0.10	0.11	0.12
α_3	26.7	23.4	21.1
Inlet guides			
r/rm	0.86	1.0	1.125
β_3	0	0	0
β_4	-31.6	-28.2	-25.9
θ	31.6	28.2	25.9
s/c	0.744	0.833	0.905
t/c	0.10	0.11	0.12
α_1	26.7	23.4	21.1

For Stage 2, the stagger of the rotor and stator blades was increased numerically by 15°.

APPENDIX II

Theory of hot wire anemometer

Let A = constant representing radiation and free convection losses from hot wire

B = constant representing the physical dimensions and properties of the hot wire and fluid

C = constant representing the heat capacity of the hot wire

H = rate of heat loss from the hot wire

H' = rate of heat storage in the hot wire

H'' = rate of electrical heating of the hot wire

I = electric current in the hot wire

I_o = electric current when fluid velocity is zero required to heat wire sufficiently to bring its resistance to mean value attained during a given set of fluctuation measurements

I_1 = electric current during fluctuation measurements

R = electrical resistance of hot wire at temperature T

R_r = electrical resistance of hot wire at reference temperature T_r

R_s = electrical resistance of hot wire at temperature of fluid stream (T_s)

T = temperature of hot wire

T_r = reference temperature in definition of temperature coefficient of resistance of hot wire

T_s = temperature of fluid stream

V = velocity of fluid stream

α = temperature coefficient of resistance of hot wire

ΔX = increment of quantity X

$\overline{X}$ = time average value of quantity X

Then, when the hot wire is immersed in the fluid stream, Reference 6 shows that the rate of loss of heat may be expressed by:-

$$H = (A + B\sqrt{V})(T - T_s) .$$

The rate of heat storage in the wire is given by:-

$$H' = \frac{CdT}{dt} .$$

The rate of electrical heat input is given by

$$H'' = I^2R$$

Then, at any instant,

$$H'' = H' + H$$

$$\text{i.e.} \qquad I^2R = \frac{CdT}{dt} + (A + B\sqrt{V})\,(T - T_s)\ .$$

If the hot wire has a small enough heat capacity, and/or the fluctuations in velocity and therefore temperature are sufficiently slow, the heat storage term may be neglected, and the equation becomes:-

$$I^2R = (A + B\sqrt{V})\,(T - T_s)$$

$$\text{Now,} \qquad R - R_s = \alpha R_r(T - T_s)$$

Thus, substituting for $(T - T_s)$,

$$\frac{I^2R \cdot \alpha R_r}{R - R_s} = A + B\sqrt{V}$$

To find the effect of a small change in V, we differentiate, remembering that for the present tests

$$I = I_1 = \text{constant}$$

$$\text{Then } I_1^{\,2}\,\alpha R_r \left[\frac{R - (R - R_s)}{(R - R_s)^2}\right] = -B \cdot \tfrac{1}{2} V^{-\frac{1}{2}} \frac{dV}{dR}\ .$$

For establishing the relationship between dV and dR it is sufficient to substitute $\bar{R}$ for R and $\bar{V}$ for V.

$$\text{Then} \qquad \frac{-I_1^{\,2}\,\alpha R_r}{\left[\bar{R}/R_s - 1\right]^2} \cdot \frac{dR}{R_s} = \frac{B}{2}\,\frac{\sqrt{\bar{V}}}{\bar{V}}\,dV\ .$$

In order to simplify this expression, we introduce the current I_o, which is the value required at zero fluid velocity to bring the resistance of the hot wire to the mean value observed during the flow fluctuation measurements. It is conveniently measured at the end of a given set of tests.

$$\text{Then,} \qquad \frac{I_o^{\,2}\,\bar{R}\,\alpha R_r}{\bar{R} - R_s} = A + 0$$

$$\text{and thus} \qquad \frac{I_1^{\,2}\,\bar{R}\,\alpha R_r}{\bar{R} - R_s} = \frac{I_o^{\,2}\,\bar{R}\,\alpha R_r}{\bar{R} - R_s} + B\sqrt{\bar{V}}$$

$$(I_1^2 - I_o^2)\, R_r\, a\, \frac{\bar{R}}{\bar{R} - R_s} = B\sqrt{\bar{V}} .$$

Therefore, substituting for $B\sqrt{\bar{V}}$,

$$\frac{-2 I_1^2\, a\, R_r}{\left[\bar{R}/R_s - 1\right]^2} \cdot \frac{dR}{R_s} = \frac{dV}{\bar{V}} \cdot (I_1^2 - I_o^2)\, R_r\, a\, \frac{\bar{R}}{\bar{R} - R_s}$$

$$\text{i.e.} \quad \frac{dV}{\bar{V}} = \frac{-2 I_1^2}{I_1^2 - I_o^2} \cdot \frac{d\,R/\bar{R}}{(\bar{R}/R_s - 1)}$$

$$\text{i.e.} \quad \frac{dV}{\bar{V}} = \frac{-dR}{\bar{R}} \cdot \frac{-2 I_1^2}{I_1^2 - I_o^2} \quad \frac{1}{(\bar{R}/R_s - 1)}$$

This is a linear relationship between $\frac{dV}{\bar{V}}$ and $\frac{dR}{\bar{R}}$. In the tests, the value of $\frac{dR}{\bar{R}}$ is indicated by the measured voltage across the hot wire and the current.

For large fluctuations, it is not sufficient to consider differentials. Instead, we consider finite increments on the time average values of V and R. In order to make the algebra more tractable, we neglect the constant A. This is permissible when the radiation and free convection losses are small compared with the forced convection losses.

Then, $$\frac{I_1^2\, \bar{R}\, a\, R_r}{\bar{R} - R_s} = B\sqrt{\bar{V}}$$

and $$\frac{I_1^2\, (\bar{R} + \Delta R)\, a\, R_r}{\bar{R} + \Delta R - R_s} = B\sqrt{\bar{V}} + \Delta V .$$

Then, $$\frac{(\bar{R} + \Delta R)\,(\bar{R} - R_s)}{(\bar{R} + \Delta R - R_s)\,(\bar{R})} = \sqrt{\frac{\bar{V} + \Delta V}{\bar{V}}}$$

$$\text{i.e.} \quad \frac{\Delta V}{\bar{V}} = \frac{\left(1 + \frac{\Delta R}{\bar{R}}\right)^2 \left(1 - \frac{R_s}{\bar{R}}\right)^2}{\left(1 + \frac{\Delta R}{\bar{R}} - \frac{R_s}{\bar{R}}\right)^2} - 1 .$$

Thus the relationship $\frac{\Delta V}{\bar{V}}$ and $\frac{\Delta R}{\bar{R}}$ is not linear.

When the frequency and/or the heat capacity of the wire are relatively high, the heat storage term can no longer be neglected. It has the effect of reducing the amplitude of the resistance fluctuations as compared with the low frequency or steady state value, and also of introducing a phase retardation. It is discussed in detail in References 7, 8 and 9. For small fluctuations it can be shown that the amplitude is reduced in the ratio $1/\sqrt{1 + 4\pi^2 f^2 M^2}$ where f is the frequency and M is a function of the wire resistance, the temperature coefficient of resistance and the heating current. The phase retardation is $\tan^{-1} 2\pi fM$.

Methods of compensation for the heat storage effect are discussed in References 7, 8 and 9. In the present tests, it is considered that the effect became serious at frequencies above about 500 c/sec. The fundamental stall cell frequencies were approximately 9 and 27 c/sec for one and three cells respectively, while the blade wake frequency was about 1500 c/sec. As explained in the text, the distortion from the amplifier system completely outweighed that from the heat storage effect in the present tests.

FIG.1

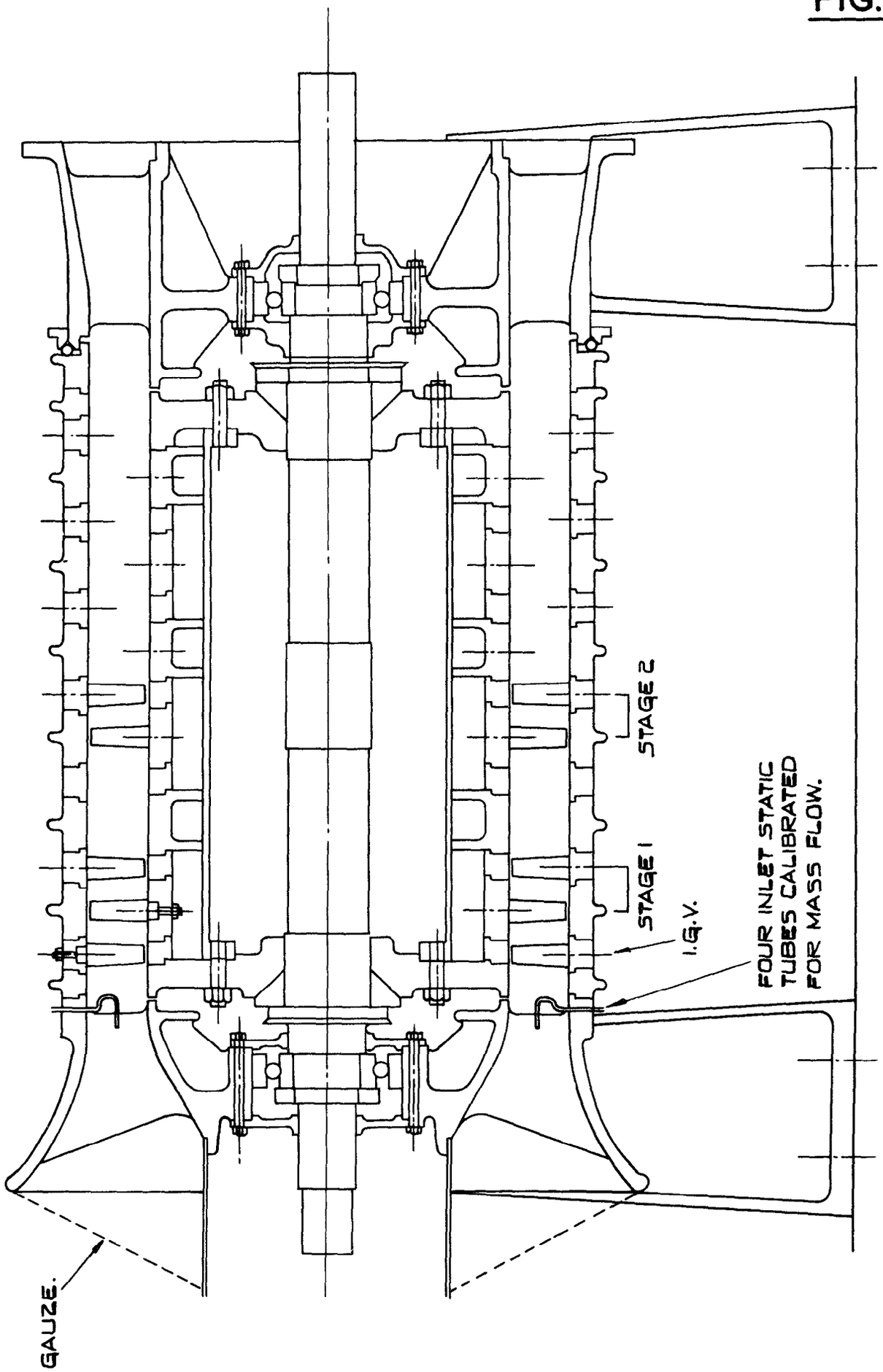

ASSEMBLY OF COMPRESSOR.

BLADE SPACING AND ANEMOMETER POSITIONS.

ARROWS INDICATE ANEMOMETER POSITIONS.

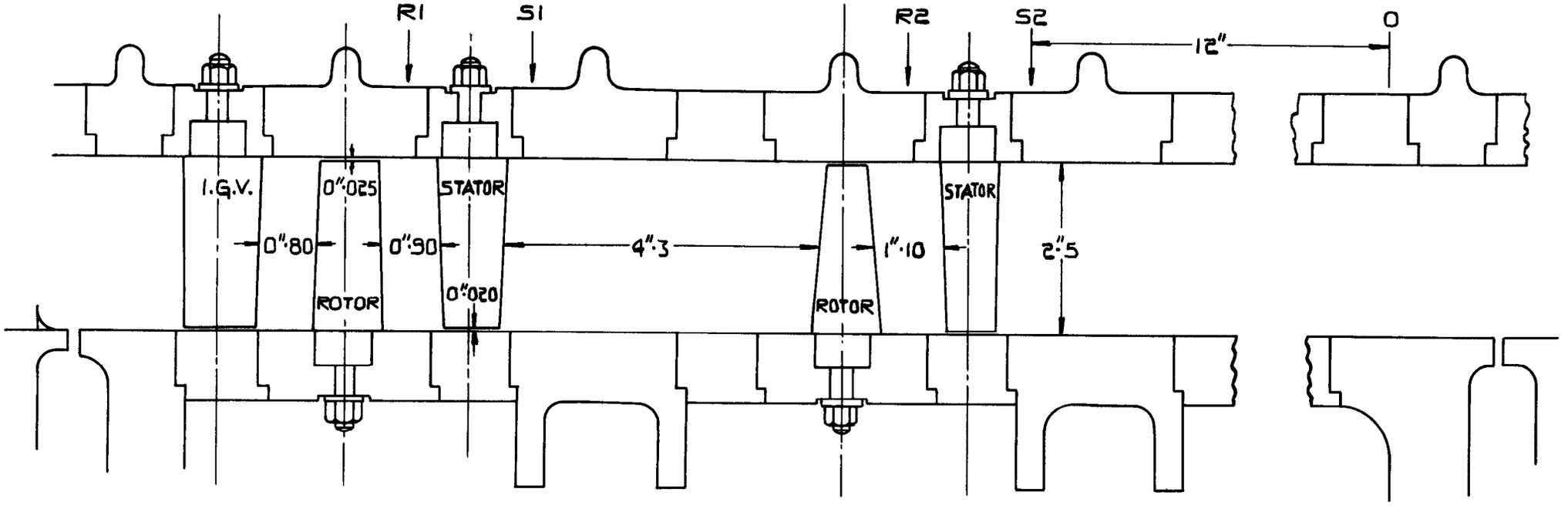

STAGE 1 STAGE 2

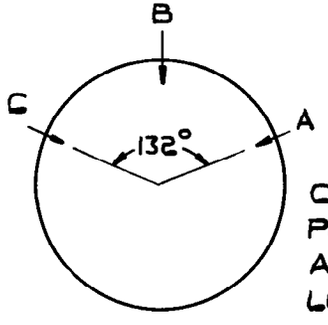

CIRCUMFERENTIAL POSITIONS OF ANEMOMETERS VIEWED LOOKING DOWNSTREAM.

NOTE STAGE 2 ROTOR AND STATOR BLADES WERE SIMILAR TO THOSE OF STAGE 1 BUT WERE INCREASED IN STAGGER BY 15°.

FIG. 2

FIG. 3

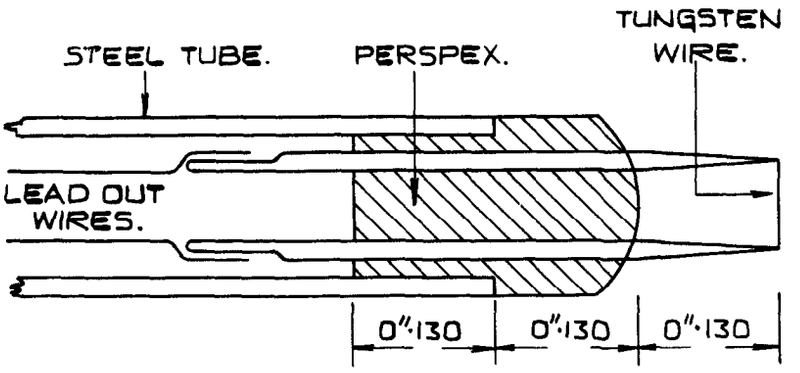

ANEMOMETER.

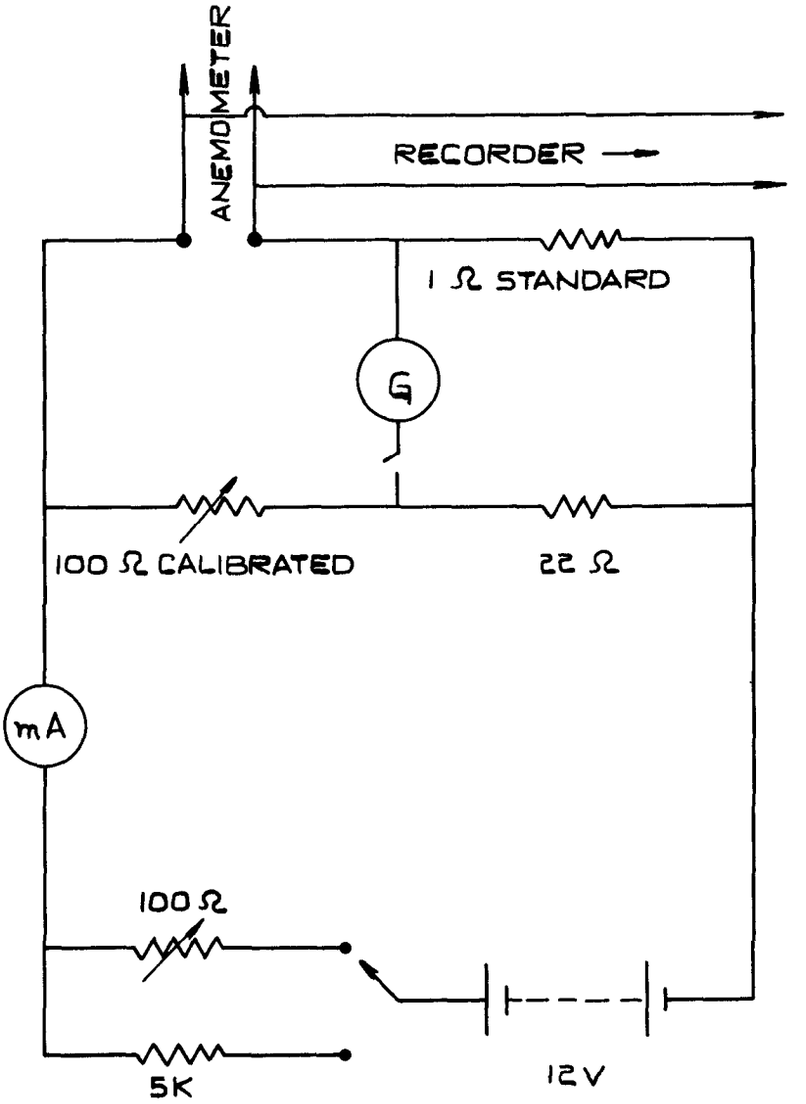

SUPPLY CIRCUIT

CIRCUIT AND ANEMOMETER DETAILS.

FIG. 4

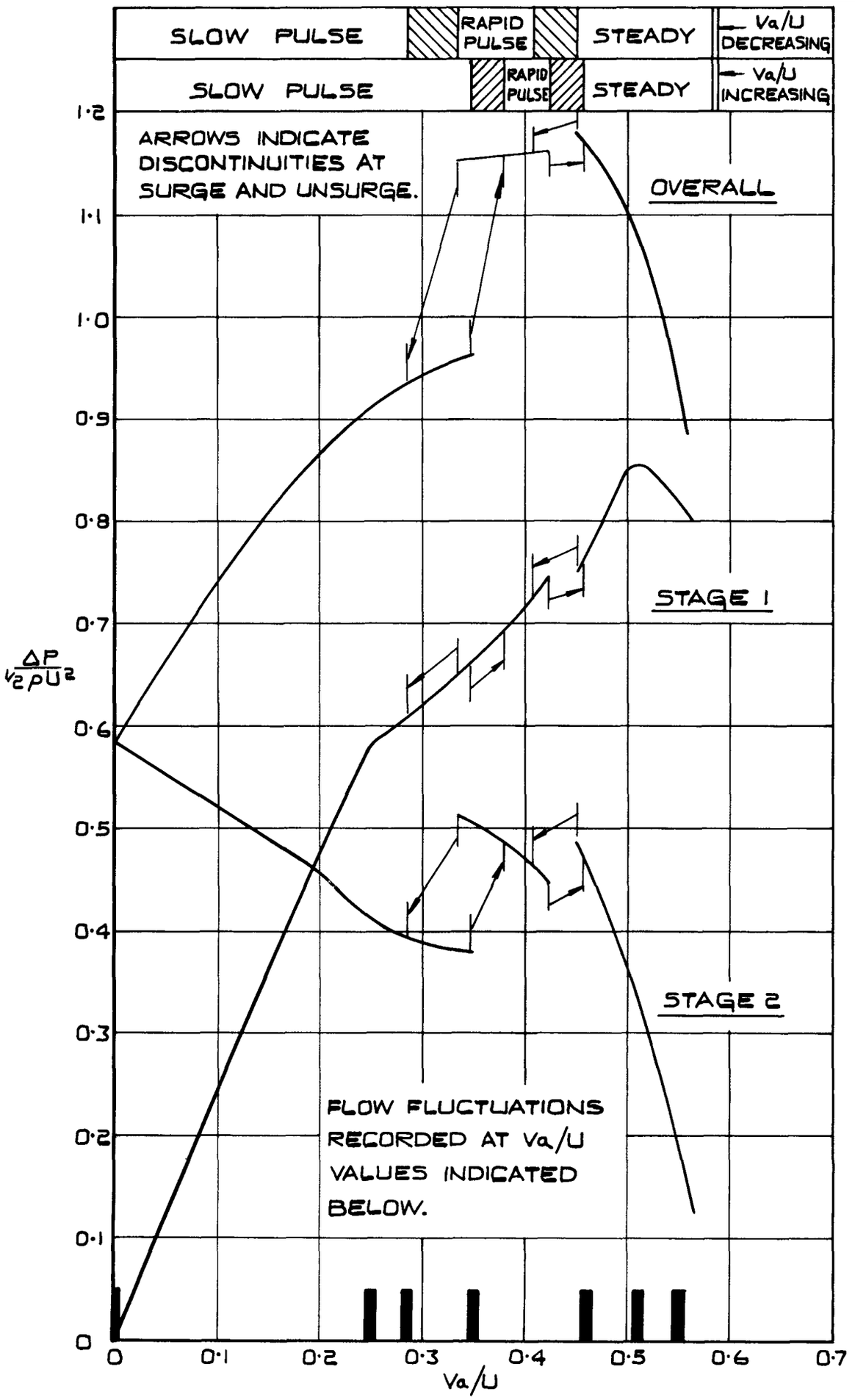

CHARACTERISTICS
STAGES TESTED IN SERIES.

FIG.5

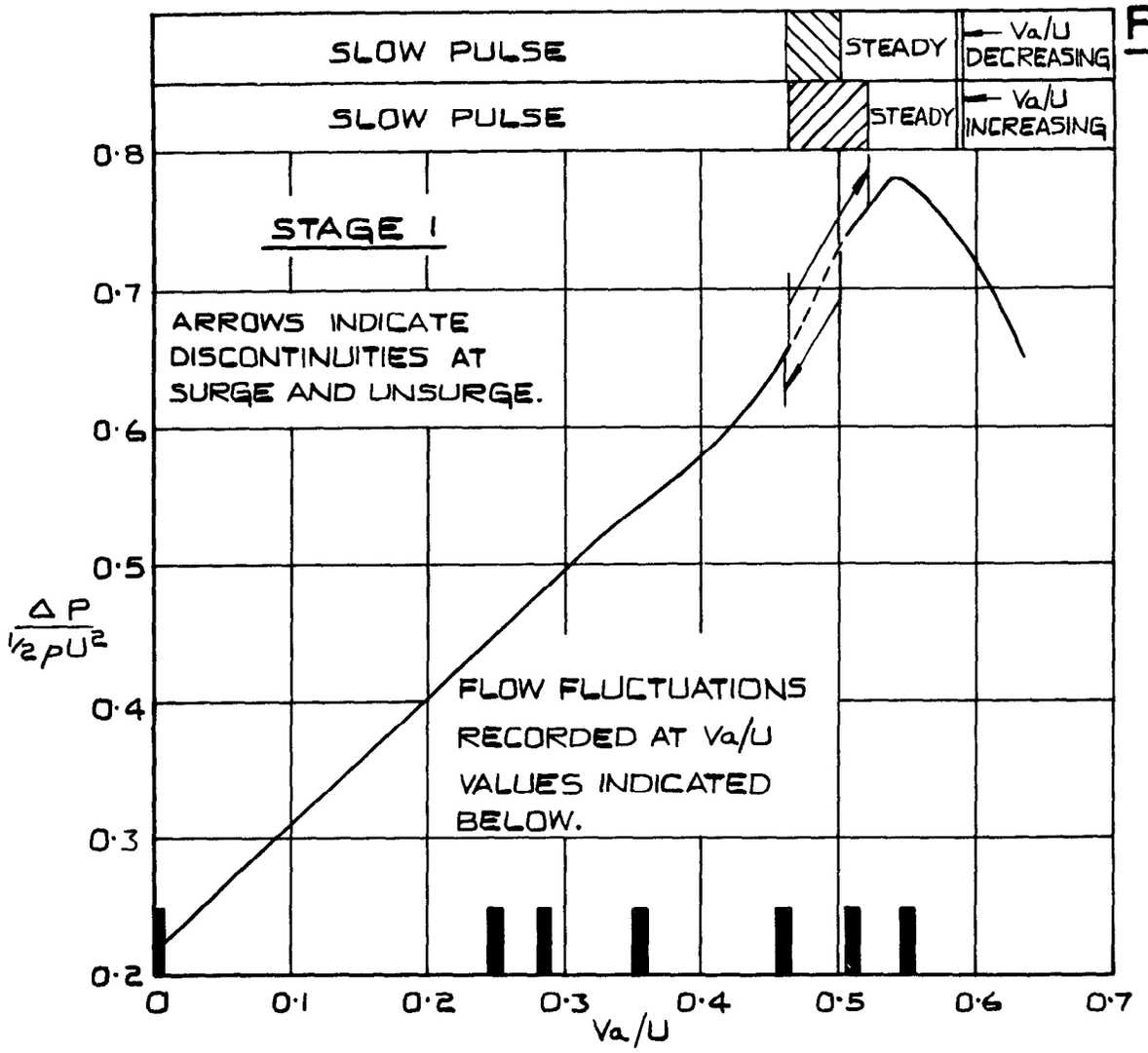

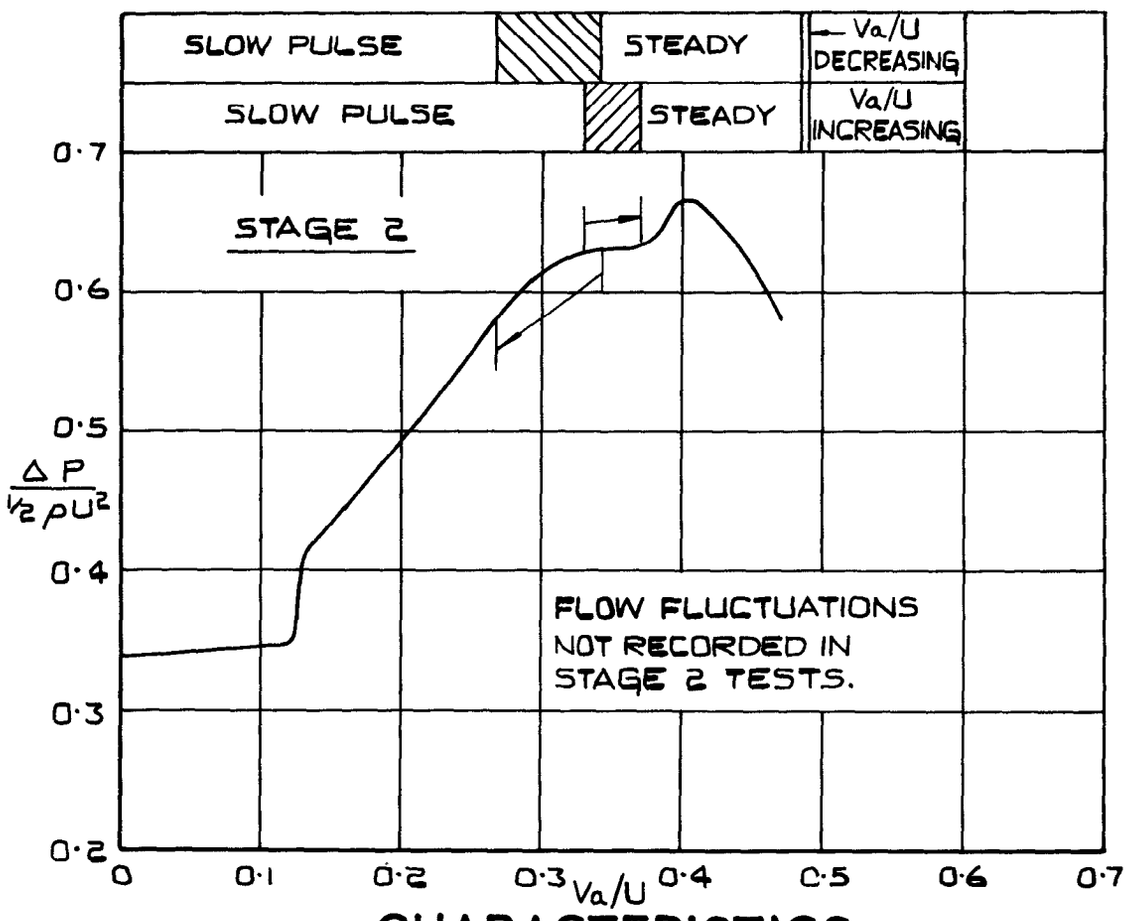

CHARACTERISTICS
STAGES TESTED SEPARATELY.

FIG. 6

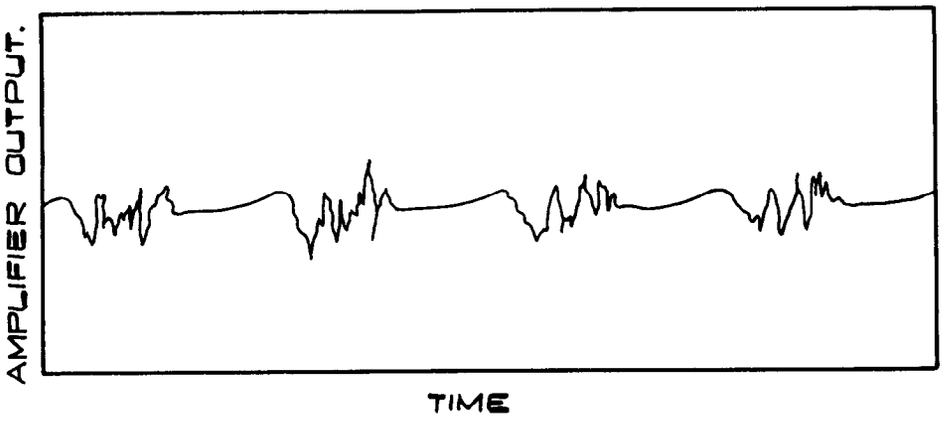

TYPICAL STALL CELL RECORD

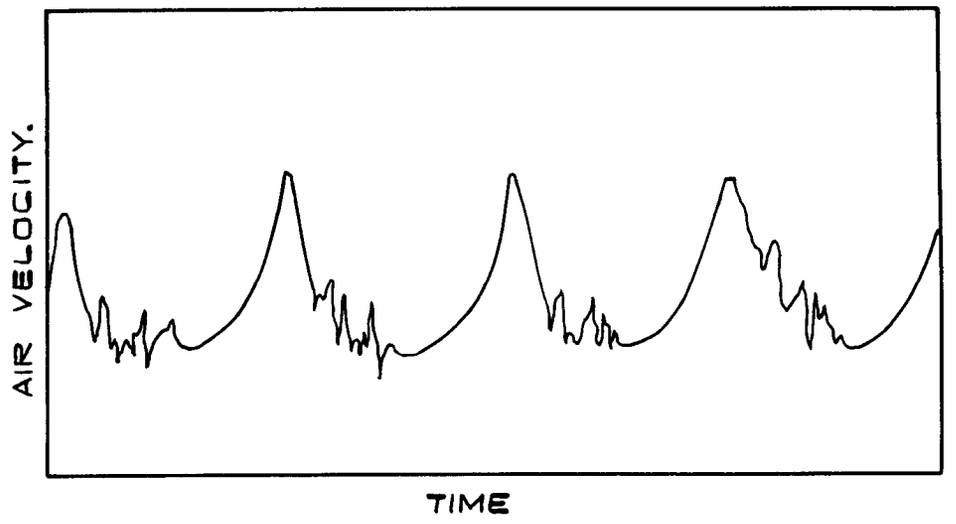

TYPICAL STALL CELL RECORD CORRECTED FOR FREQUENCY DISTORTION.

NOTE NO CORRECTION MADE FOR PHASE-SHIFT OF HIGH FREQUENCY COMPONENTS.

EFFECT OF AMPLIFIER DISTORTION ON TYPICAL STALL CELL RECORD.

FIG.7

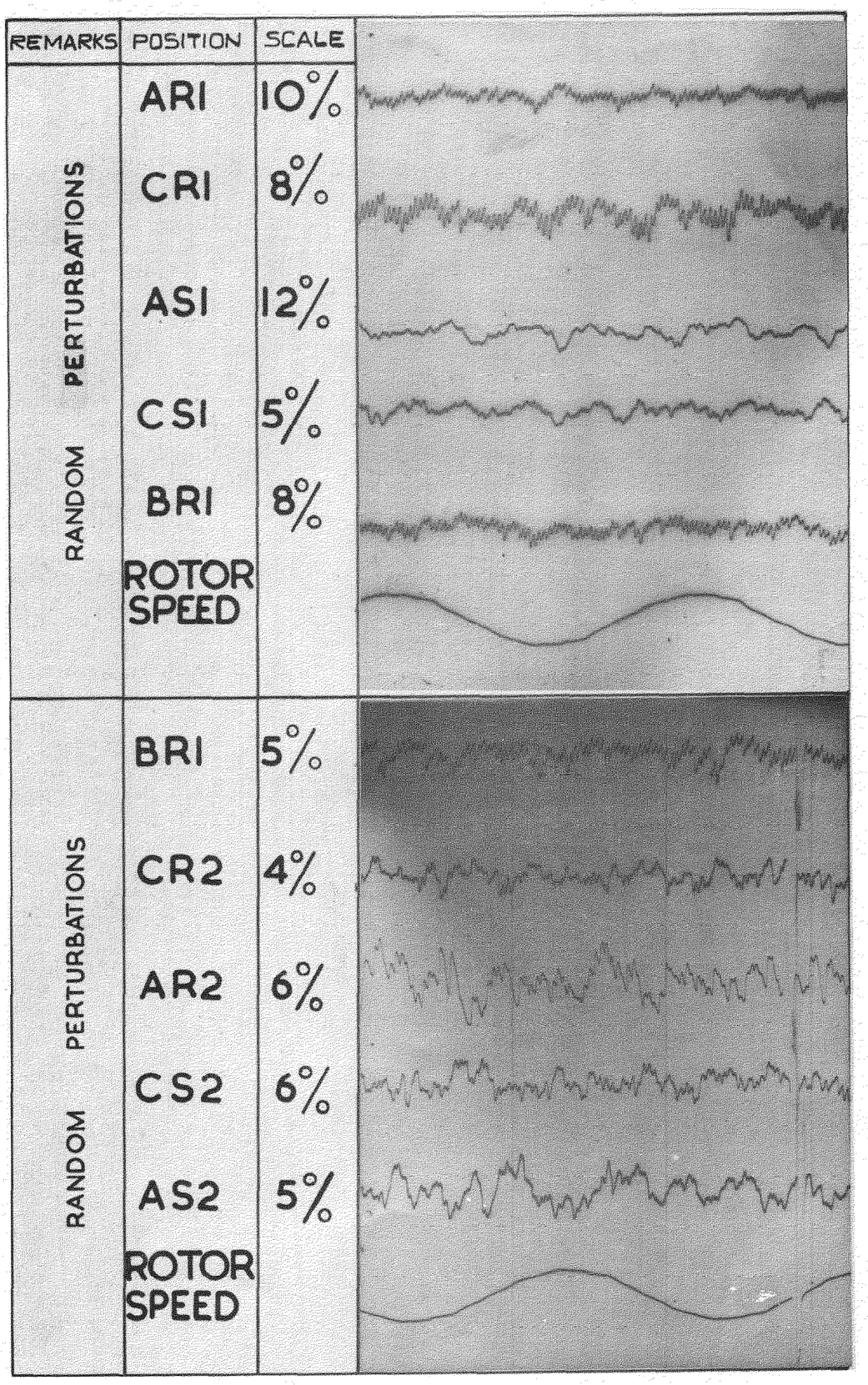

THE SCALES ARE EXPRESSED AS % OF THE MEAN AXIAL VELOCITY PER 0"·5 ON THE RECORDS.

ANEMOMETER RECORDS- TWO STAGE BUILD.

$V_a/U = 0.55$

FIG. 8

REMARKS	POSITION	SCALE
RANDOM PERTURBATIONS.	AR1	5%
	CR1	8%
	AS1	9%
	CS1	5%
	BR1	8%
	ROTOR SPEED	
RANDOM PERTURBATIONS	BR1	4%
	CR2	4%
	AR2	6%
	CS2	7%
	AS2	5%
	ROTOR SPEED	

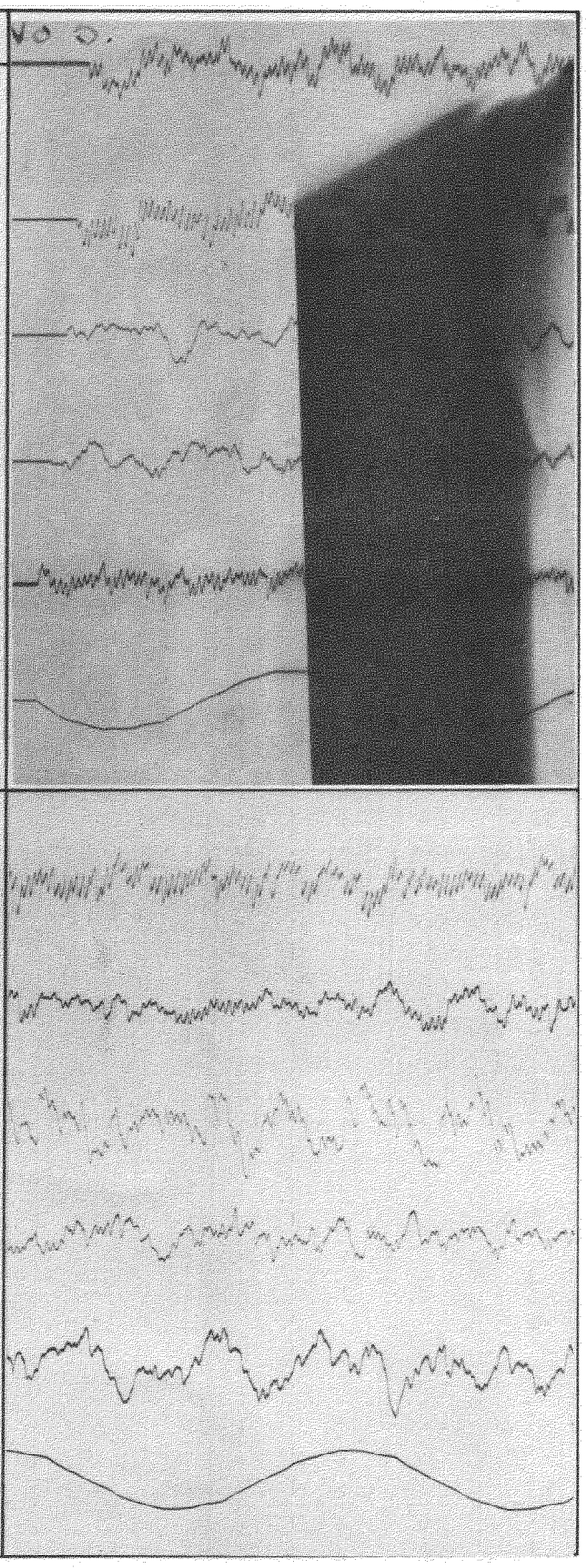

THE SCALES ARE EXPRESSED AS % OF THE MEAN AXIAL VELOCITY PER 0"·5 ON THE RECORDS.

ANEMOMETER RECORDS – TWO STAGE BUILD.

$V_a/U = 0{\cdot}51$

FIG. 9

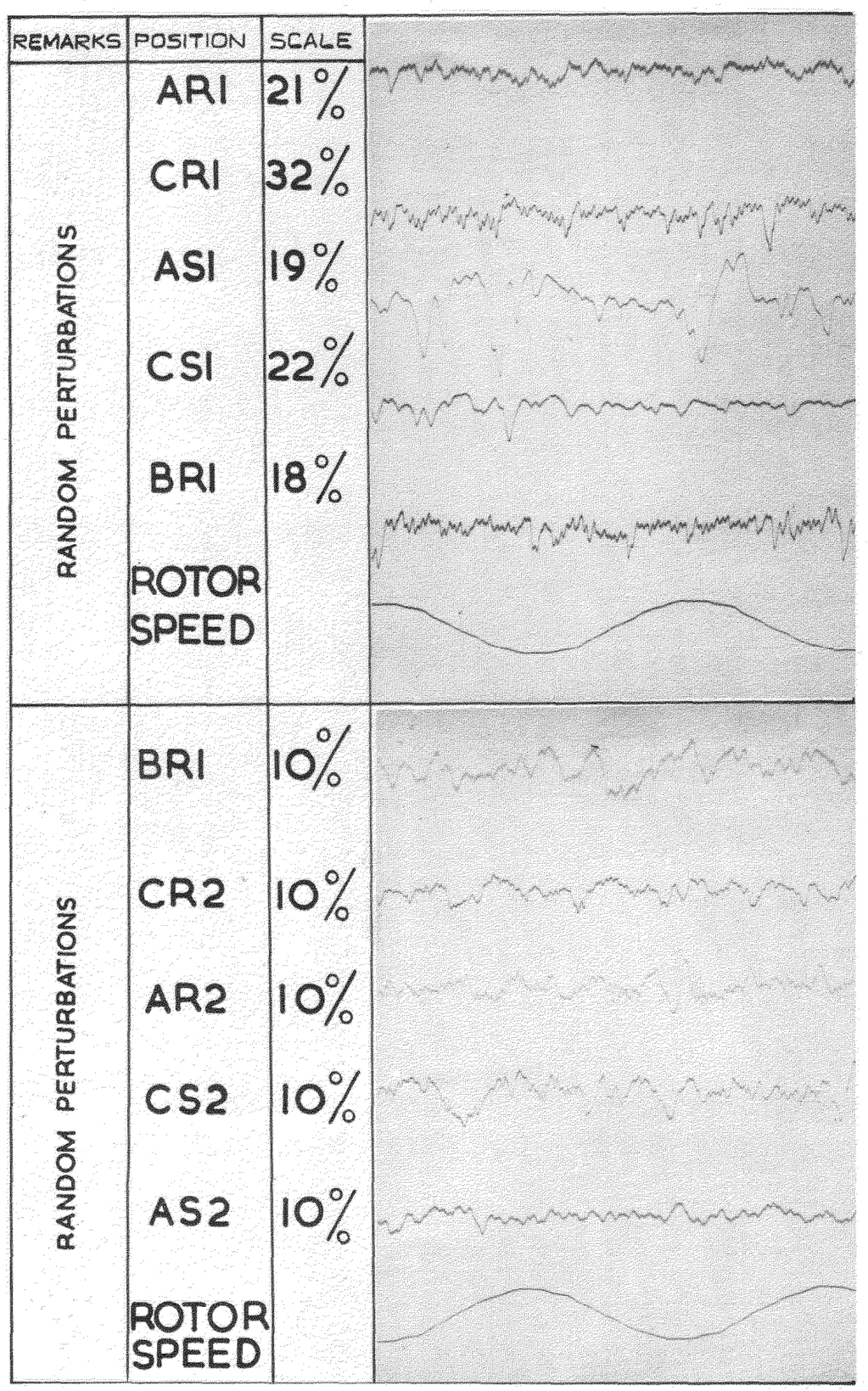

THE SCALES ARE EXPRESSED AS % OF THE MEAN AXIAL VELOCITY PER 0·5" ON THE RECORDS.

ANEMOMETER RECORDS-TWO STAGE BUILD.

$V_a/U = 0{\cdot}46$

FIG.10

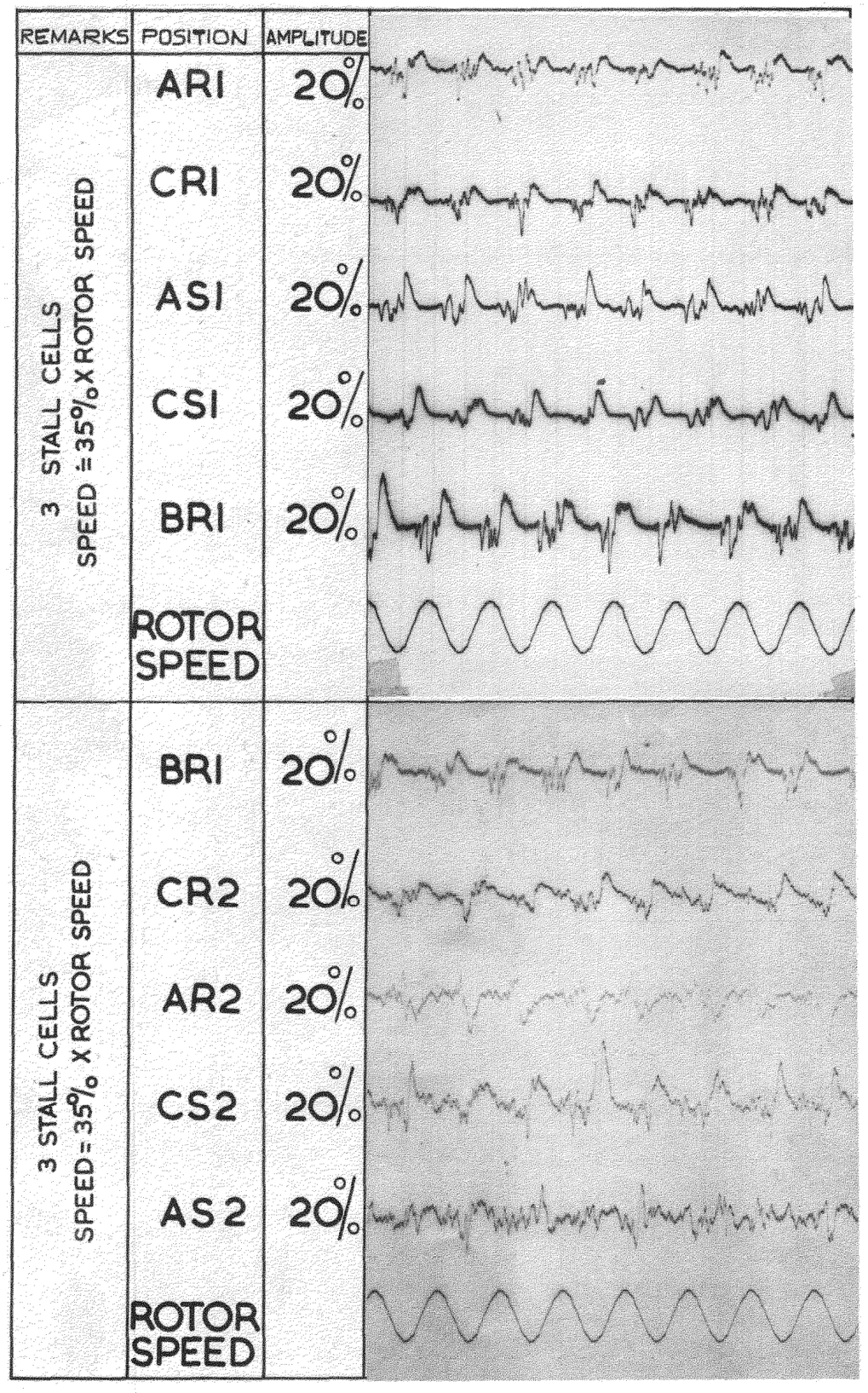

AMPLITUDES ARE EXPRESSED AS % OF THE MEAN AXIAL VELOCITY AND REFERS TO THE LOW FREQUENCY COMPONENTS.

ANEMOMETER RECORDS - TWO STAGE BUILD

$V_a/U = 0.35$

FIG. 11

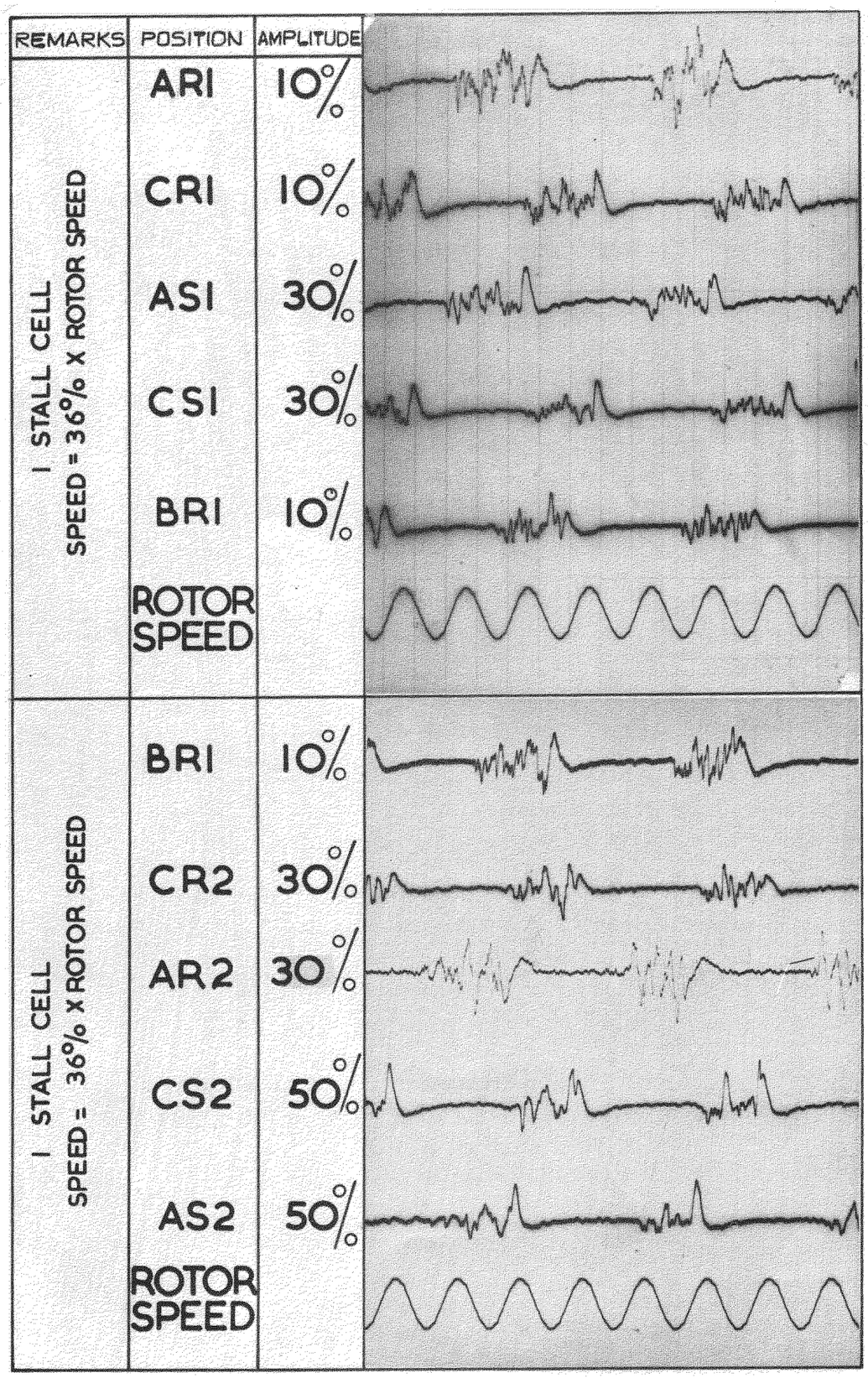

AMPLITUDES ARE EXPRESSED AS % OF THE MEAN AXIAL VELOCITY AND REFER TO THE LOW FREQUENCY COMPONENT.

ANEMOMETER RECORDS - TWO STAGE BUILD

$V_a/U = 0.285$

FIG. 12

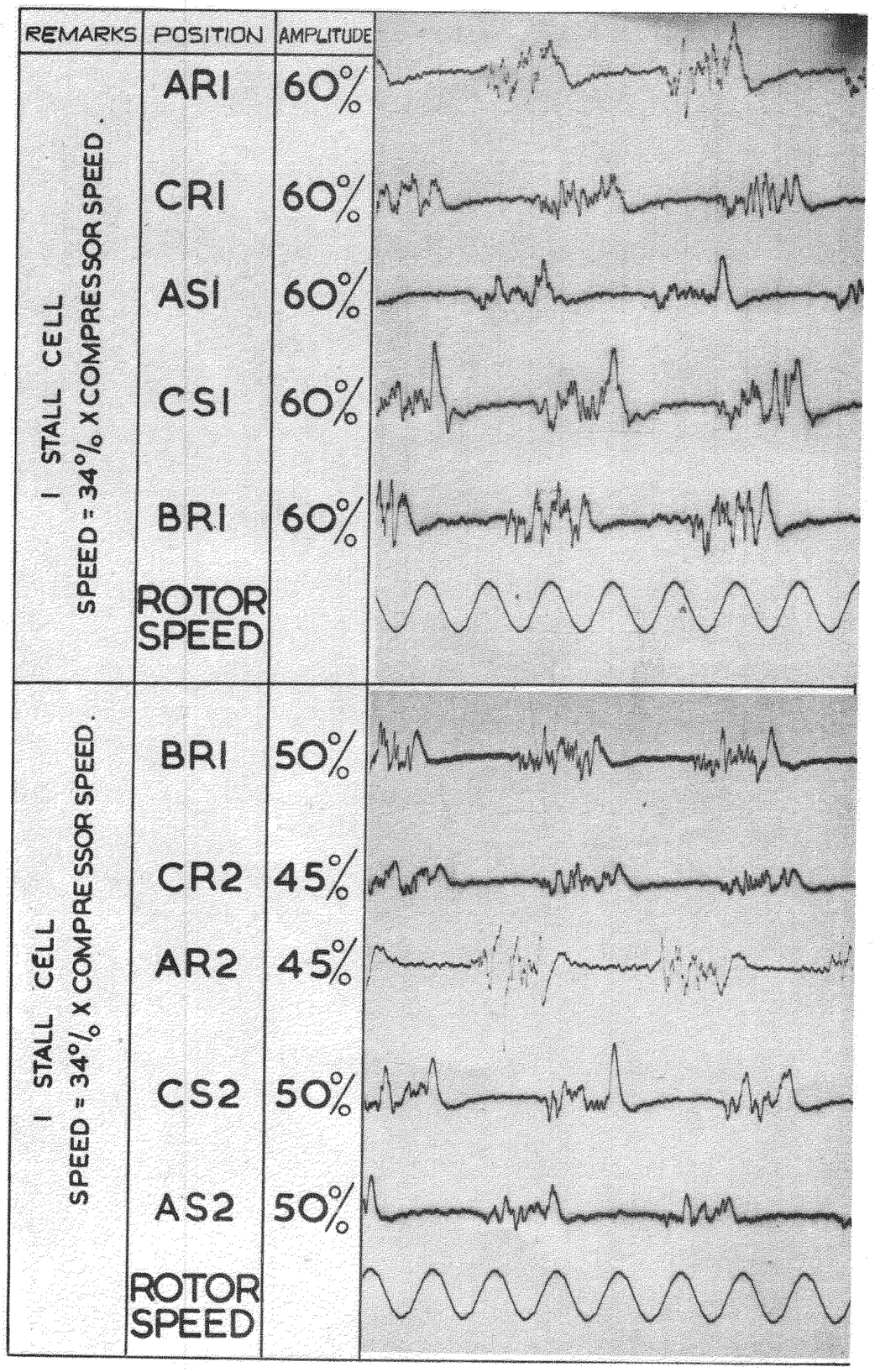

AMPLITUDES ARE EXPRESSED AS % OF THE MEAN AXIAL VELOCITY AND REFER TO THE LOW FREQUENCY COMPONENT.

ANEMOMETER RECORDS – SINGLE STAGE BUILD.

Va/U = 0·285 AND 0·25.

FIG.13

REMARKS	POSITION	AMPLITUDE
RANDOM PERTURBATIONS.	AR1	35-40
	CR1	35-40
	AS1	35-40
	CS1	35-40
	BR1	35-40
	ROTOR SPEED	
RANDOM PERTURBATIONS.	BR1	35-40
	CR2	35-40
	AR2	35-40
	CS2	35-40
	AS2	35-40
	ROTOR SPEED	

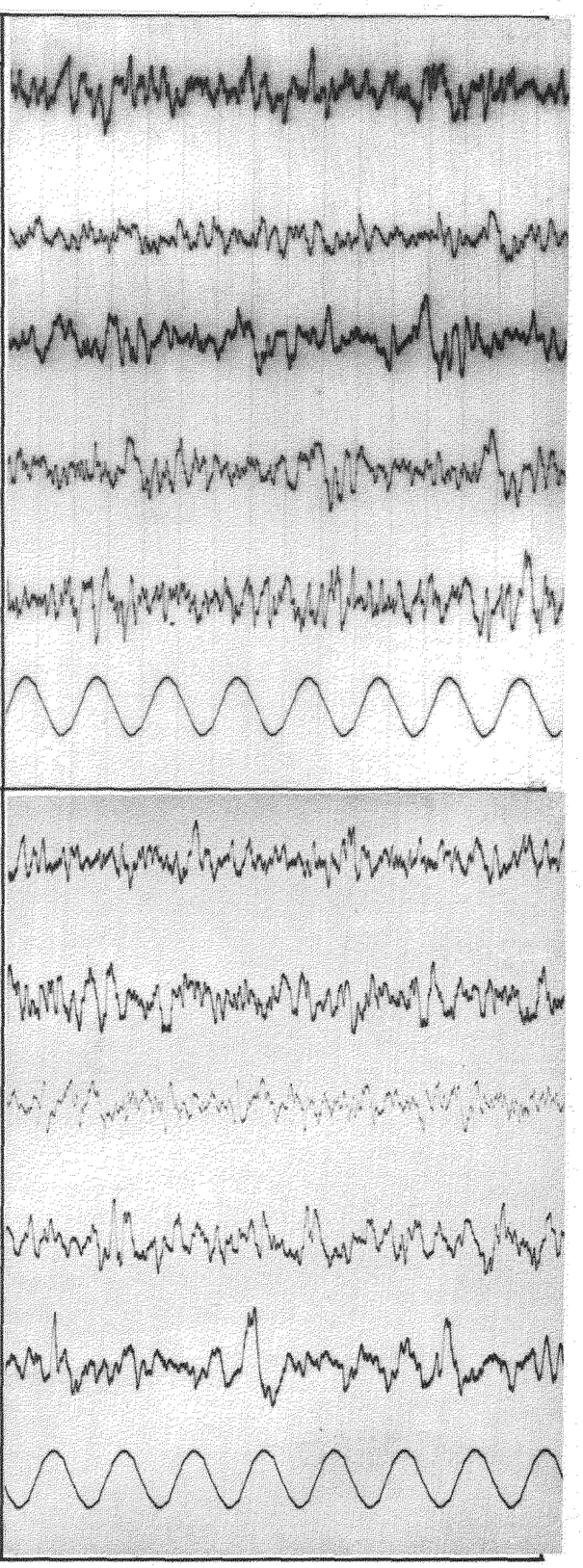

AMPLITUDES ARE EXPRESSED AS % OF MEAN AXIAL VELOCITY.

ANEMOMETER RECORDS- SINGLE STAGE BUILD.

$V_a/U=0$

FIG.14

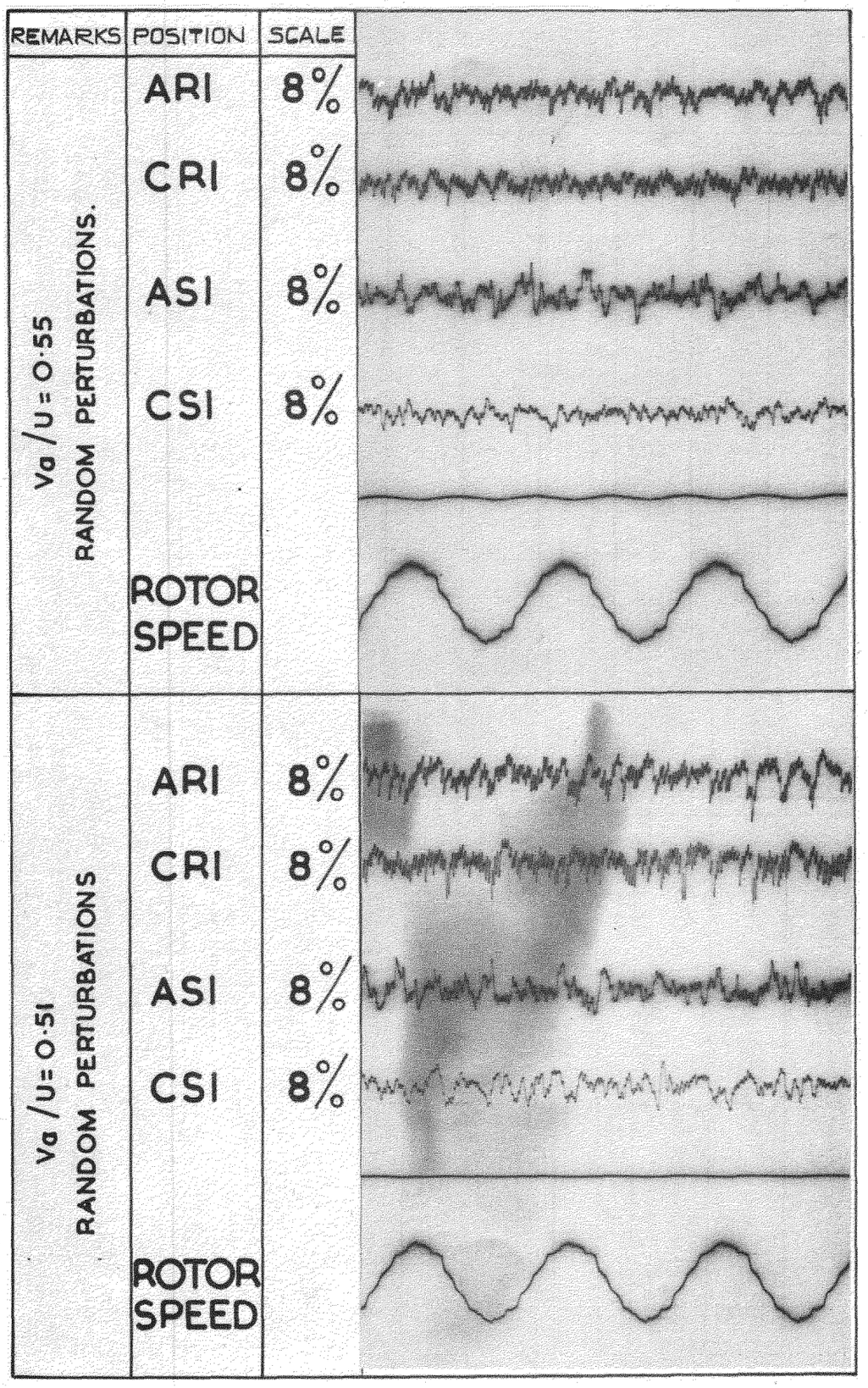

THE SCALES ARE EXPRESSED AS % OF THE MEAN AXIAL VELOCITY PER 0·5" ON THE RECORDS.

ANEMOMETER RECORDS- SINGLE STAGE BUILD.

V_a/U=0·55 AND 0·51

FIG.15

REMARKS	POSITION	AMPLITUDE
$V_a/U = 0.46$ 1 STALL CELL SPEED = 35% X ROTOR SPEED	A RI	50%
	C RI	50%
	A SI	50%
	C SI	50%
	ROTOR SPEED	
$V_a/U = 0.35$ 1 STALL CELL SPEED = 36% X ROTOR SPEED	A RI	65%
	C RI	73%
	A SI	59%
	C SI	62%
	ROTOR SPEED	

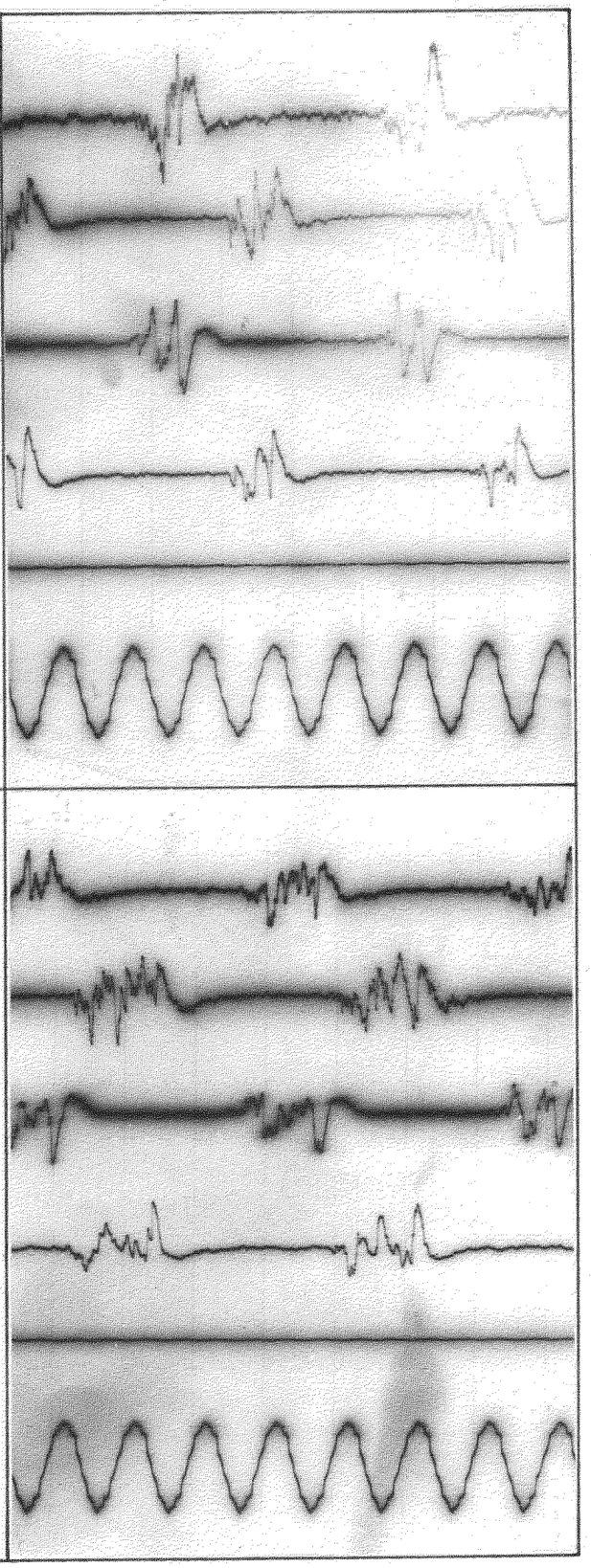

AMPLITUDES ARE EXPRESSED AS % OF THE MEAN AXIAL VELOCITY AND REFER TO THE LOW FREQUENCY COMPONENT.

ANEMOMETER RECORDS - SINGLE STAGE BUILD

$V_a/U = 0.46$ AND 0.35

FIG.16

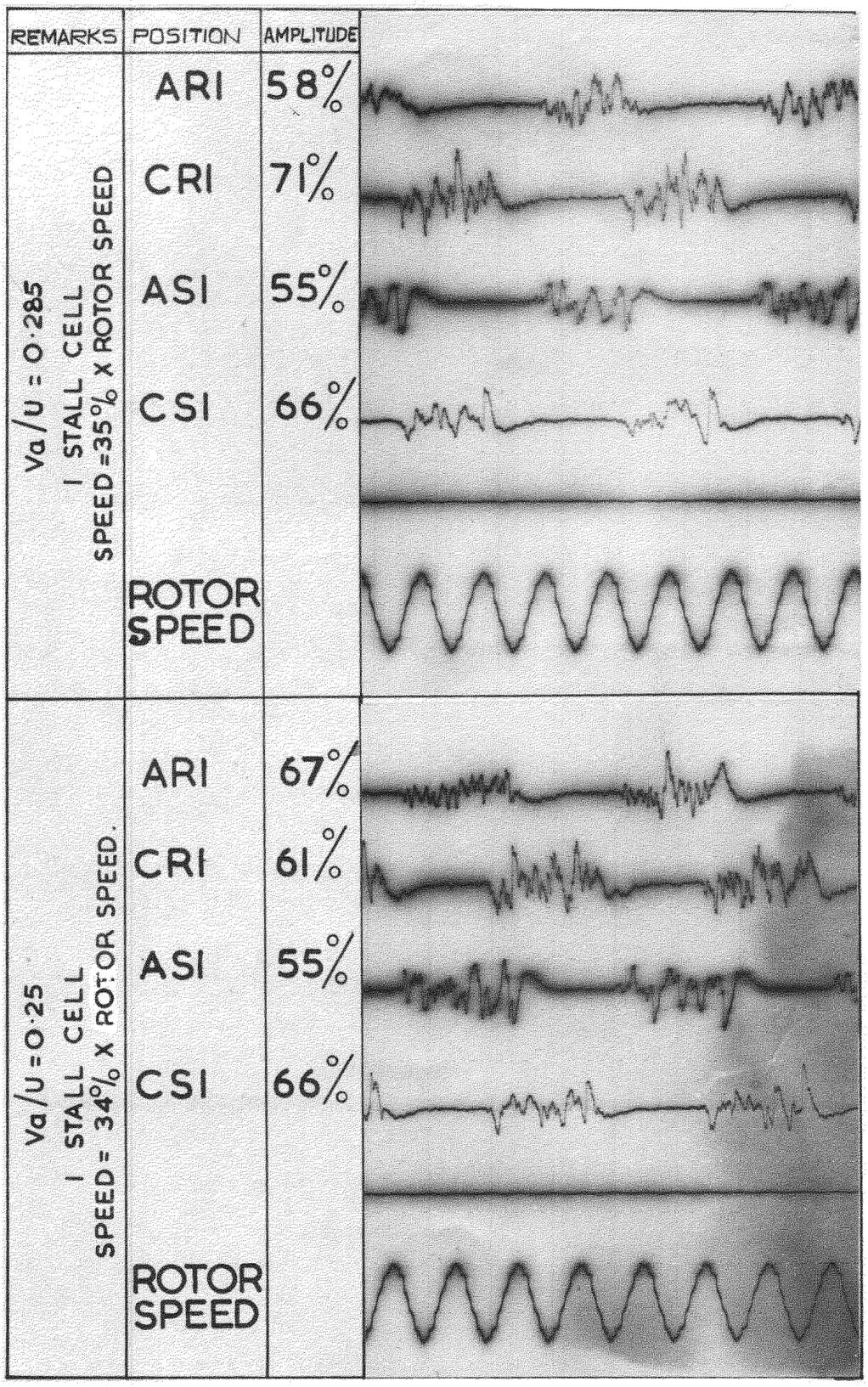

AMPLITUDES ARE EXPRESSED AS % OF THE MEAN AXIAL VELOCITY AND REFER TO THE LOW FREQUENCY COMPONENT.

ANEMOMETER RECORDS - TWO STAGE BUILD.

Va/U = 0·25.

FIG.17

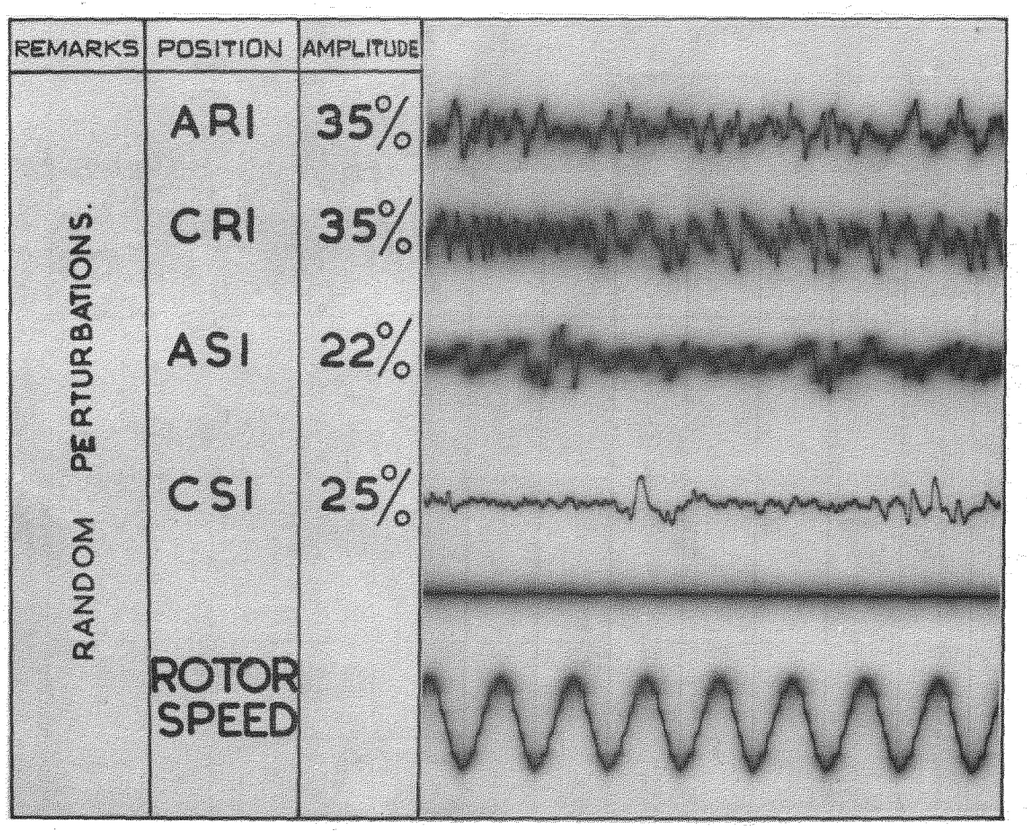

AMPLITUDES ARE EXPRESSED AS % OF THE MEAN AXIAL VELOCITY

ANEMOMETER RECORDS - TWO STAGE BUILD

$V_a/U = 0$

FIG.18

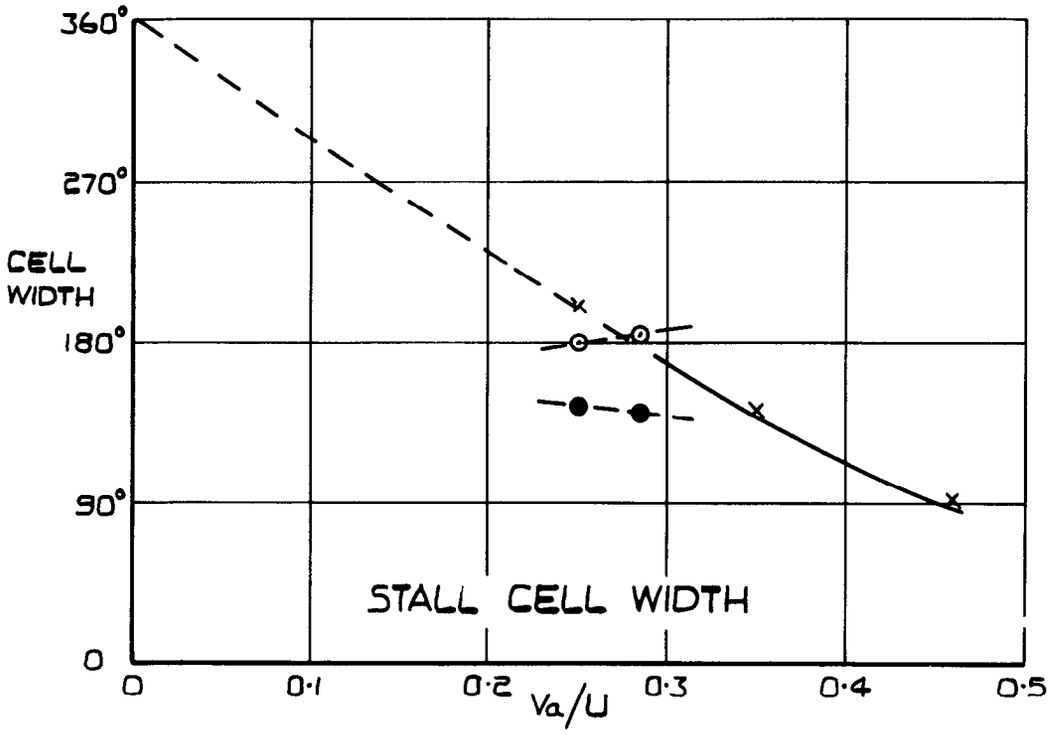

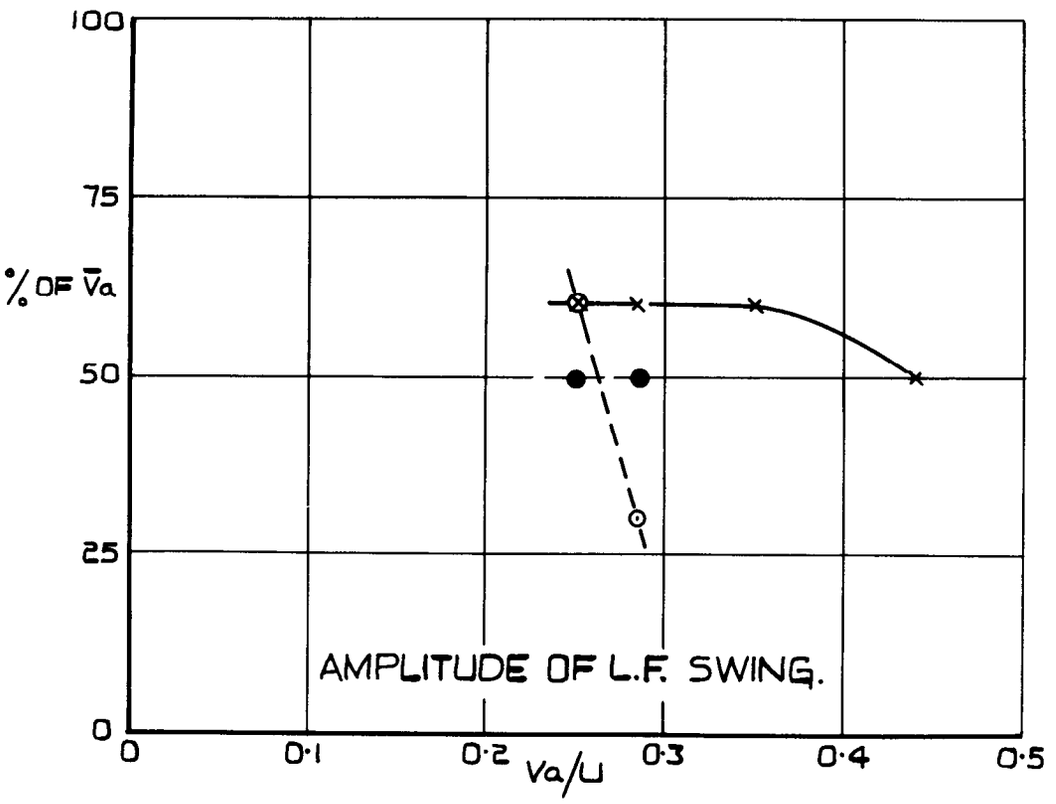

× – SINGLE STAGE TESTS, AFTER STATORS.
⊙ – TWO STAGE TESTS, AFTER FIRST STATORS.
● – TWO STAGE TESTS, AFTER SECOND STATORS.

STALL CELL CHARACTERISTICS OF SLOW PULSE SURGE.

FIG.19

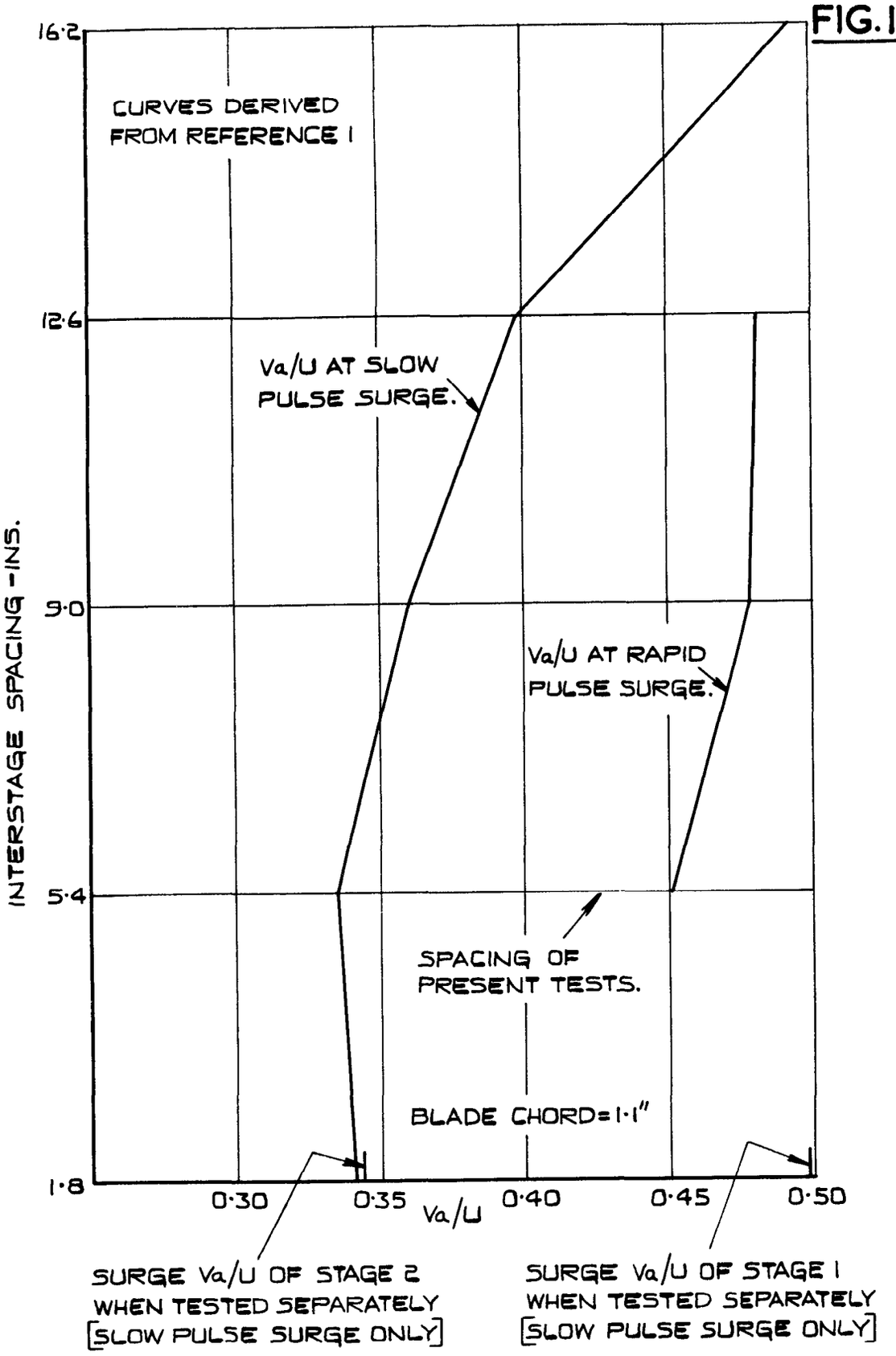

TWO STAGE TESTS
EFFECT OF INTERSTAGE SPACING ON SURGE FLOW COEFFICIENT.

C.P. No. 449
(19,900)
A.R.C. Technical Report

Printed and published by
HER MAJESTY'S STATIONERY OFFICE

To be purchased from
York House, Kingsway, London W.C.2
423 Oxford Street, London W.1
13A Castle Street, Edinburgh 2
109 St Mary Street, Cardiff
39 King Street, Manchester 2
Tower Lane, Bristol 1
2 Edmund Street, Birmingham 3
80 Chichester Street, Belfast
or through any bookseller

Printed in England

S.O. Code No. 23-9011-49

C.P. No. 449